Exceptional Event Demonstration for Ozone Exceedances in Clark County, Nevada: August 6–7, 2018

September 2021

Clark County Department of Environment and Sustainability
4701 West Russell Road, Suite 200
Las Vegas, NV 89118
(702) 455-5942

TABLE OF CONTENTS

LIST OF FIGURES

LIST OF TABLES

1.0 OVERVIEW

1.1 INTRODUCTION

Ozone (O_3) exceedances in Clark County are frequently influenced by surrounding wildfires. In the proper weather conditions, wildfire emissions can travel hundreds of miles from the point of origin. This is especially true of wildfires in California, which cause more exceedances of the National Ambient Air Quality Standard (NAAQS) for ozone in Clark County than fires in other areas because of regionally predominant winds that flow from California to the Las Vegas Valley (LVV) in summer.

Figure 1-1 uses data from annual "Wildland Fire Summary" reports (2014–2018) from the National Interagency Coordination Center (NICC) to show the strong relationship between the number of ozone exceedance days in Clark County and the total area in California burned by wildfires ($R^2 = 0.9091$). The 2018 fire season in California was the most destructive on record, with the NICC reporting a total of 8,054 fires burning an area of 1,823,153 acres. Figure 1-2 shows the high correlation between the area burned (logarithmic value) in California and the number of ozone exceedance days in Clark County from May to August 2018 ($R^2 = 0.9591$), based on the "2018 Wildfire Activity Statistics" report published by the California Department of Forestry and Fire Protection (CAL FIRE). Though it represents only the areas of the state for which CAL FIRE was responsible, that was more than 50% of the total burned area in California.

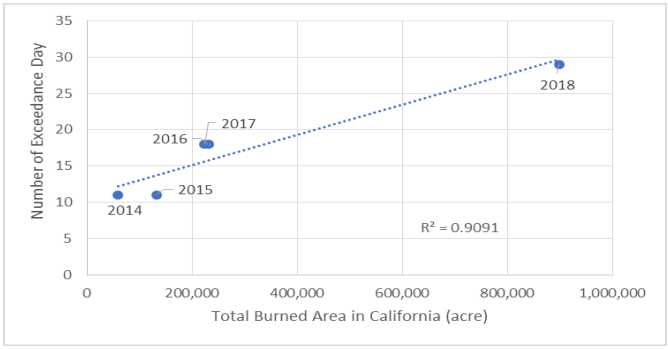

Figure 1-1. Relationship between Total Burned Area in California and Number of Exceedance Days in Clark County in Summer Months (May–August) 2014–2018.

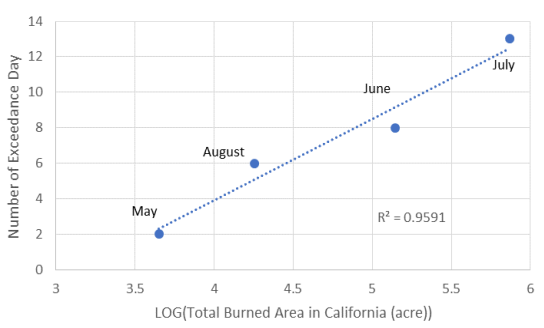

Figure 1-2. Relationship between Log Value of Total Burned Area and Number of Exceedance Days in Summer Months of 2018.

With that background in mind, the Clark County Department of Environment and Sustainability (DES) is concurrently submitting several exceptional events demonstrations of ozone concentrations that exceeded the 2015 ozone NAAQS due to smoke impact on the days in 2018 listed in Table 1-1. All have been prepared consistent with Title 40, Part 50 of the Code of Federal Regulations (40 CFR 50).

This document is submitted for the August 6-7, 2018, event influenced by smoke from the Ferguson Fire, Lions Fire, Carr Fire, Donnell Fire, and Mendocino Complex Fire.

The submittal process began with an Exceptional Events Initial Notification sent to EPA Region 9 on November 30, 2020 (Appendix A). With this demonstration package, DES petitions the Regional Administrator for Region 9 of the U.S. Environmental Protection Agency (EPA) to exclude air quality monitoring data for ozone on August 6–7, 2018, from the normal planning and regulatory requirements under the Clean Air Act (CAA) in accordance with the Exceptional Events Rule (EER), codified at 40 CFR 50.1, 50.14, and 51.930.

Table 1-1 lists the maximum daily 8-hour average of ozone (MDA8 ozone) at network monitors on the exceedance days.

Table 1-1. Ozone Monitors Proposed for Data Exclusion

AQSID[1]	320030043	320030071	320030073	320030075	320030298	320030540
Date	**Paul Meyer**	**Walter Johnson**	**Palo Verde**	**Joe Neal**	**Green Valley**	**Jerome Mack**
20180619[2]	72 (10)	72 (14)	—	—	77 (4)	75 (4)
20180620	71 (15)	74 (9)	—	72 (10)	—	—
20180623	72 (7)	76 (4)	71 (5)	72 (9)	75 (6)	72 (10)
20180627	75 (4)	76 (4)	72 (3)	72 (8)	78 (1)	76 (3)
20180714	72 (13)	—	—	—	78 (3)	78 (1)
20180715	—	71 (21)	—	78 (2)	73 (11)	73 (7)
20180716	75 (3)	79 (1)	75 (1)	80 (1)	71 (19)	73 (8)
20180717	74 (5)	77 (3)	74 (2)	—	—	—
20180725	71 (17)	72 (15)	—	—	72 (14)	—
20180726	72 (8)	75 (6)	70 (6)	—	77 (4)	77 (2)
20180727	72 (9)	74 (11)	70 (7)	76 (4)	—	—
20180730	—	—	—	—	73 (11)	72 (11)
20180731	—	73 (13)	—	73 (6)	—	—
20180806	79 (1)	77 (2)	72 (4)	76 (3)	74 (10)	71 (12)
20180807	73 (6)	74 (7)	—	74 (5)	72 (16)	71 (13)

[1]Air Quality System identification numbers (AQSID) and local names identify key monitors.
[2]MDA8 ozone is listed in parts per billion (ppb) with Tier 2, Key Factor 2 ranking of measurement for 2018 season in parentheses.

1.2 EXCEPTIONAL EVENT DEMONSTRATION CRITERIA

40 CFR 50.1(j) states:

> *Exceptional event* means an event(s) and its resulting emissions that affect air quality in such a way that there exists a clear causal relationship between the specific event(s) and the monitored exceedance(s) or violation(s), is not reasonably controllable or preventable, is an event(s) caused by human activity that is unlikely to recur at a particular location or a natural event(s), and is determined by the Administrator in accordance with 40 CFR 50.14 to be an exceptional event.

40 CFR 50.14(c)(1)(i) requires that air agencies must "notify the public promptly whenever an event occurs or is reasonably anticipated to occur which may result in the exceedance of an applicable air quality standard" in accordance with the mitigation requirement at 40 CFR 51.930(a)(1). Details on DES's public notification can be found in Appendix B.

As specified in 40 CFR 50.14(c)(3)(iv), the following elements must be included to justify the exclusion of air quality data from a NAAQS determination:

1. A narrative conceptual model that describes the event(s) causing the exceedance or violation and a discussion of how emissions from the event(s) led to the exceedance or violation at the affected monitor(s).

2. A demonstration that the event affected air quality in such a way that there exists a clear causal relationship between the specific event and the monitored exceedance or violation.

3. Analyses comparing the claimed event-influenced concentration(s) to concentrations at the same monitoring site at other times. However, the EPA Administrator is restricted from requiring a state to prove a specific percentile point in the distribution of data.

4. A demonstration that the event was both not reasonably controllable and not reasonably preventable.

5. A demonstration that the event was a human activity that is unlikely to recur at a particular location, or was a natural event.

"EPA Guidance on the Preparation of Exceptional Events Demonstration for Wildfire Events that May Influence Ozone Concentrations" (EPA 2016) describes a three-tier analysis approach to determine a "clear causal relationship" for exceptional events, which is summarized below. Section 4 of this document, "Clear Causal Relationship," provides the details of these analyses.

Tier 1:
Key factors for this tier are exceedances out of the normal ozone season and/or concentrations that are 5–10 ppb greater than non-event-related concentrations.

Tier 2:
There are two key factors for this tier: fire emissions & distance (Q/d) and comparison of event ozone concentrations to non-event high-ozone concentrations. This tier may include additional analyses of smoke maps, plume trajectories, satellite retrievals, sounding data, and time series of supporting ground measurements to provide evidence of wildfire emissions transported to local monitors.

Tier 3:
This tier involves statistical modeling of MDA8 ozone concentrations using generalized additive models (GAMs) to assess wildfire influences on local ozone concentrations.

DES has prepared this package to meet the requirements for seeking EPA concurrence for data exclusion.

This exceptional event demonstration will undergo a 30-day public comment period concurrent with EPA's review, beginning September 3, 2021. A copy of the public notice, along with any comments received and responses to those comments, will be submitted to EPA after the comment period has closed, consistent with the requirements of 40 CFR 50.14(c)(3)(v). Appendix C documents the public comment process.

1.3 REGULATORY SIGNIFICANCE OF THE EXCLUSION

The LVV, located within Clark County, Nevada, is currently designated as a nonattainment area for the 2015 ozone NAAQS of 70 ppb. Table 1-2 lists the 4th highest 8-hour average ozone recorded at the monitors listed in Table 1-1—including wildfire days in 2018 and excluding wildfire days in 2020—for the most recent three-year period (2018–2020), along with the resulting design value (DV) for each monitor. The table also shows the 4th highest 8-hour average ozone and DVs for 2018 after the requested exceedance days are excluded from the DV calculation (the shaded columns). Since the recalculated DVs meet the 2015 NAAQS, the valley would be reclassified as "attainment" if EPA concurs with this demonstration. EPA concurrence will thus have a significant impact on DES's attainment of the 2015 ozone NAAQS.

Table 1-2. Impact of Wildfire Events on Design Values of 2018–2020 (all values in ppb)

Site Name	Fourth Highest Average			Current	Wildfire Days Excluded	
	2018	2019	2020[1]	Design Value	2018	Design Value
Jerome Mack	75	66	67	69	72	68
Paul Meyer	75	69	70	71	71	70
Joe Neal	76	68	68	70	71	69
Walter Johnson	76	68	70	71	73	70
Palo Verde	72	62	67	67	68	65
Green Valley	77	70	68	71	72	70

[1] Assume wildfire days are excluded.

2.0 AREA DESCRIPTION AND CHARACTERISTICS OF NON-EVENT OZONE FORMATION

2.1 AREA DESCRIPTION

Clark County covers 8,091 square miles at the southern tip of Nevada and has a population of over 2.2 million.[1] More than 95% of the county's residents live in the Las Vegas Valley, which is part of the Mojave Desert and constitutes Hydrographic Area (HA) 212. The valley encompasses about 1,600 km^2 and is surrounded by mountains extending 2,000–10,000 feet above its floor (Figure 2-1). The valley slopes downward from west to east (approximately 900 to 500 m above mean sea level), which affects the local climatology by driving variations in wind, temperature, and precipitation.

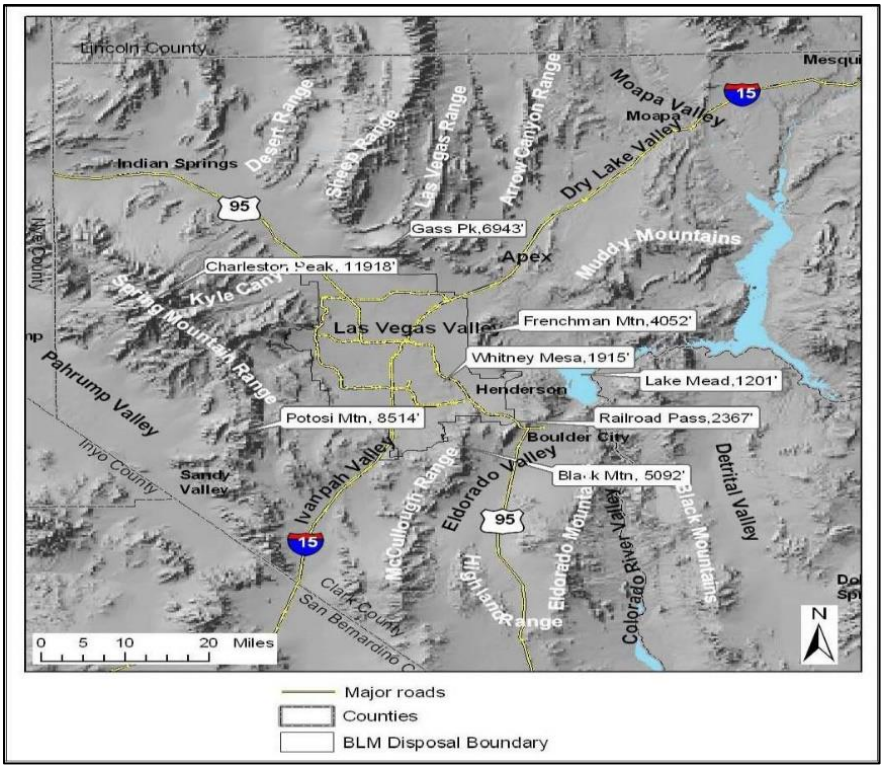

Figure 2-1. Mountain Ranges and Hydrographic Areas Surrounding the Las Vegas Valley.

Valley weather is characterized by low rainfall, hot summers, and mild winters. On average, June is the driest month; monsoons from the Gulf of California increase the humidity and cloud cover in July and August. The Interstate 15 (I-15) corridor through the Mojave Desert and Cajon Pass links Las Vegas with the eastern Los Angeles Basin, about 275 km to the southwest. This corridor is a potential pathway for the export of pollution from Los Angeles to the Mojave Desert and the LVV.

[1] *Clark County, Nevada 2017 Population Estimates*. Clark County (NV) Department of Comprehensive Planning.

Figure 2-2 shows the locations of Clark County ozone monitors. Most of the stations—Paul Meyer (PM), Walter Johnson (WJ), Palo Verde (PV), Joe Neal (JO), Jerome Mack (JM), and Green Valley (GV)—are in the populated areas of the valley (HA 212), but there are outlying stations in Apex, Mesquite, Boulder City, Jean, and Indian Springs. A station at the Spring Mountain Youth Camp was operated as a special purpose monitoring site for part of the 2018 ozone season.

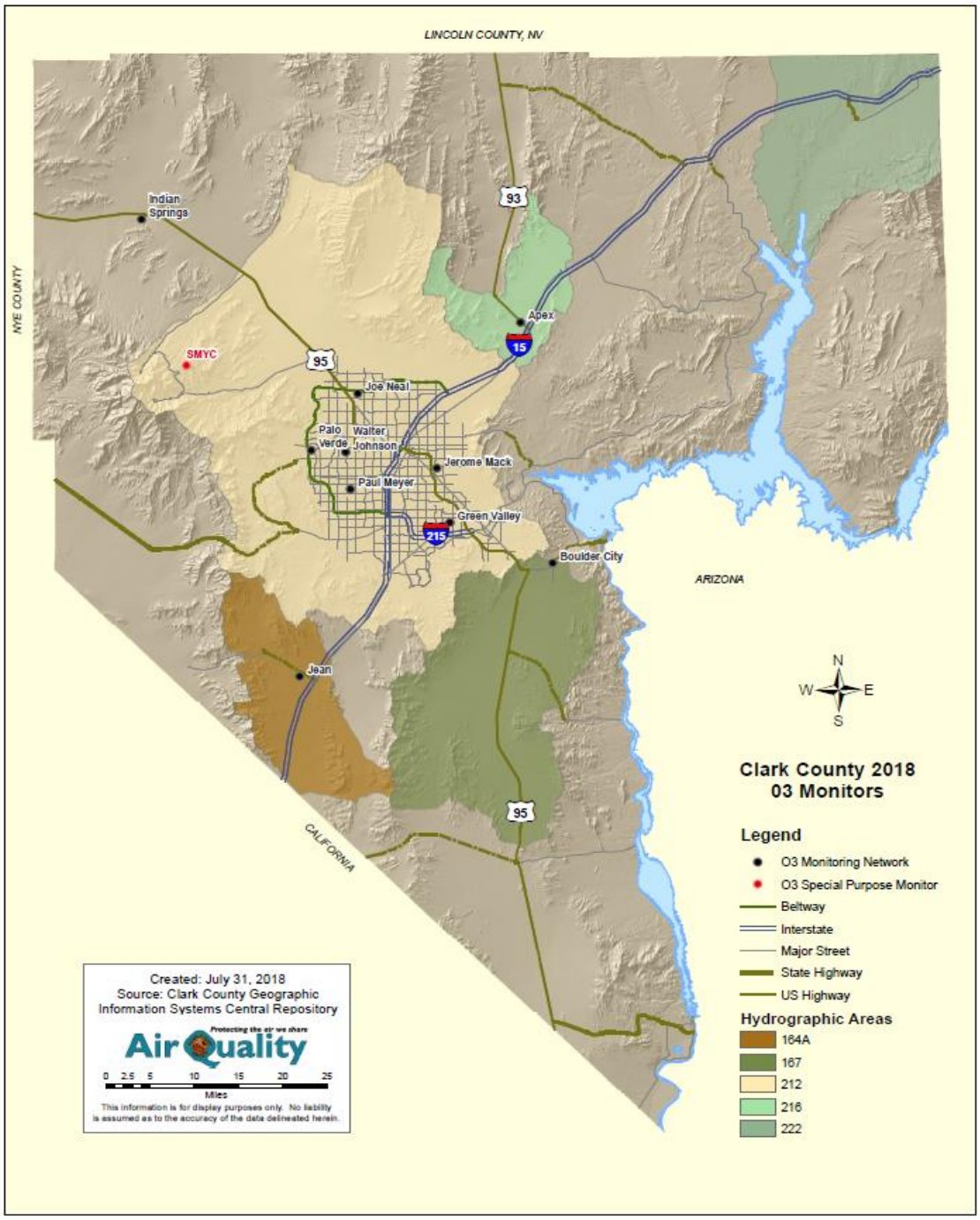

Figure 2-2. Clark County O_3 Monitoring Network.

Figures 2-3 and 2-4 show the locations of Clark County's Federal Equivalent Method (FEM) and Federal Reference Method (FRM) $PM_{2.5}$ monitors, respectively. Most of the stations are located in the populated areas of HA 212, with one outlying station in Jean, Nevada. Jean is considered a regional background site because it is located far enough from the valley to avoid impacts from local emissions. It is upwind of the LVV, but downwind of southern California.

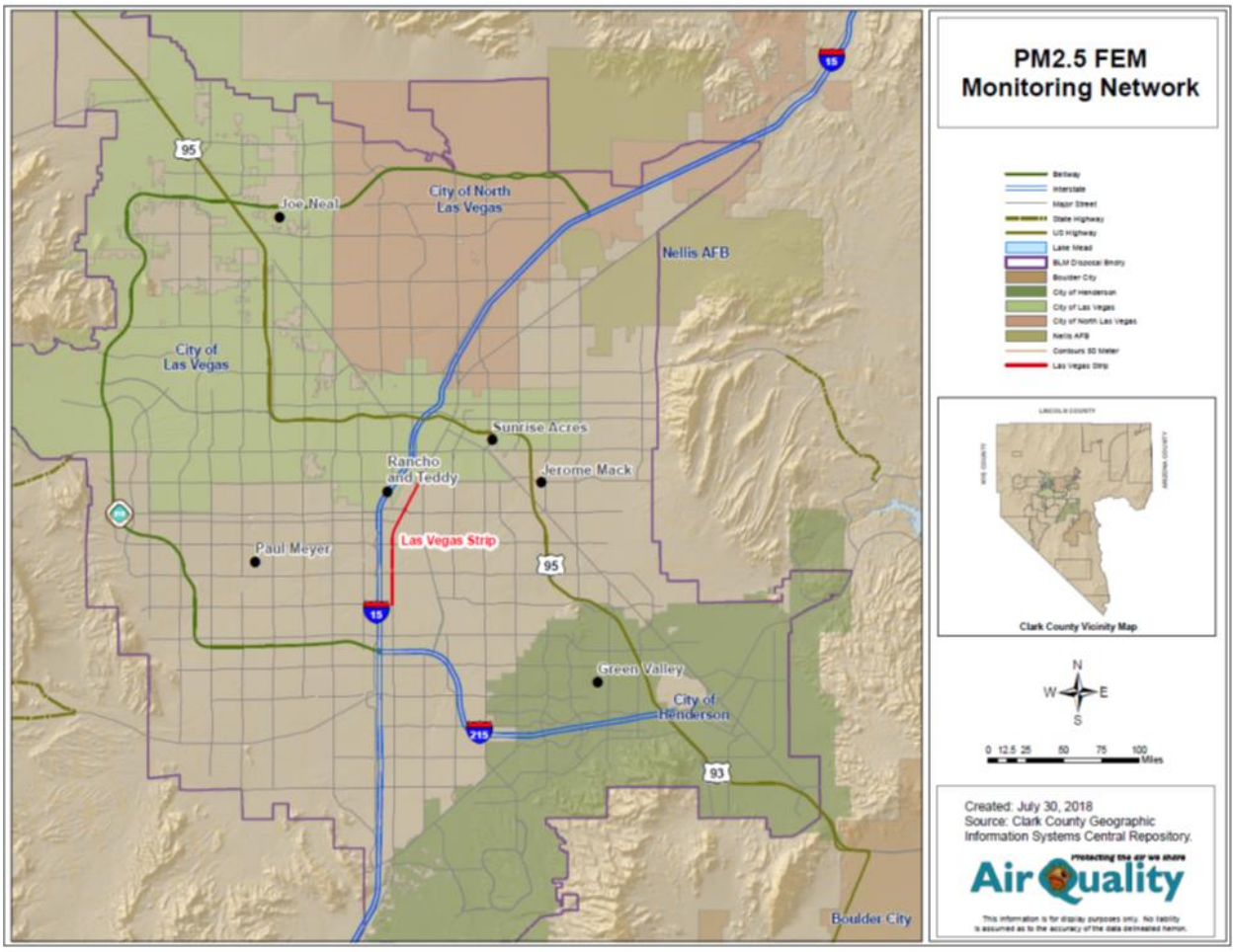

Figure 2-3. Locations of FEM $PM_{2.5}$ Monitors.

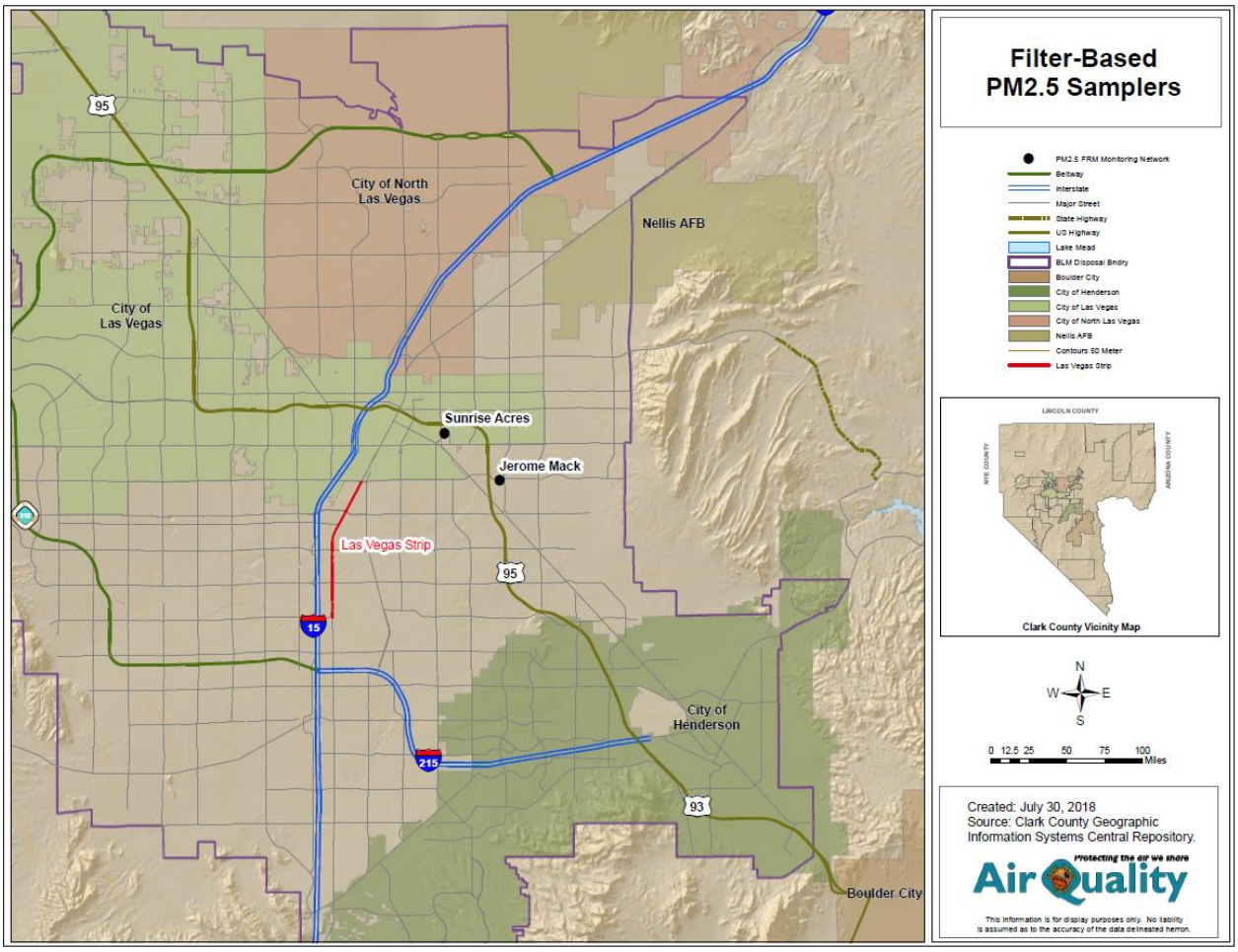

Figure 2-4. Locations of FRM $PM_{2.5}$ Monitors.

2.2 CHARACTERISTICS OF NON-EVENT OZONE FORMATION

Ozone, a secondary pollutant, is formed by complex processes in the interaction of nitrogen oxides (NO_x), volatile organic compounds (VOCs), temperature, and the intensity of solar radiation. The elevated ozone in the LVV can be characterized as the result of a combination of locally produced ozone under relatively stagnant conditions and different degrees of regional transport from upwind source areas, mainly in California.

2.2.1 Emission Trend

Mobile emission is the largest source of ozone precursors in Clark County. The area adjacent to two major transportation routes, I-15 and U.S. Highway 95, registers the highest emissions in the LVV. Figures 2-5 and 2-6 illustrate the county's ozone planning inventory for NO_x and VOC emissions, respectively, on a typical summer weekday. Throughout the years, ozone has decreased dramatically across much of the eastern United States over the last two decades (He et al.

2013; Lefohn et al. 2010), largely as a result of stricter emission controls on stationary and mobile NO_x sources (Butler et al. 2011; EPA 2012). These same reductions can be seen in California and Clark County.

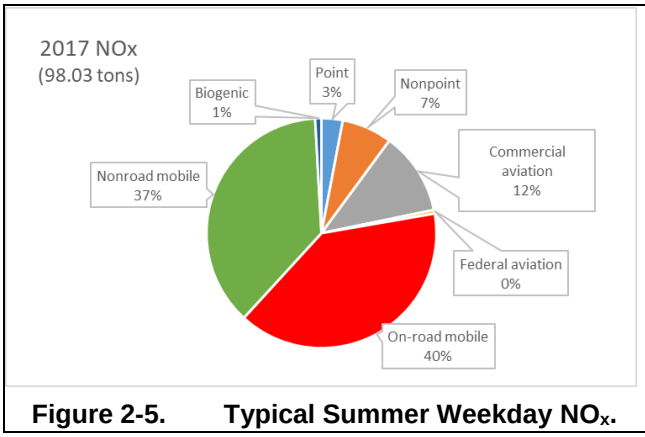

Figure 2-5. Typical Summer Weekday NO_x.

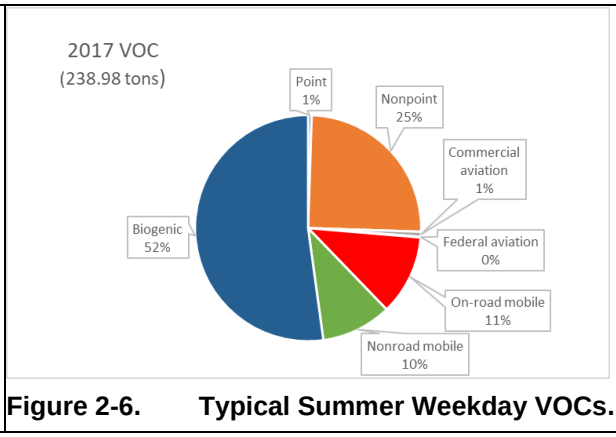

Figure 2-6. Typical Summer Weekday VOCs.

Source: https://www.clarkcountynv.gov/Environmental%20Sustainability/SIP%20Related%20Documents/O3/20200901_2015_O3_EI_ES_SIP_with_Appendices.pdf?t=1619706653363.

Figure 2-7 shows the downward trends of NO_x and VOC anthropogenic emissions in California from 1990–2019.

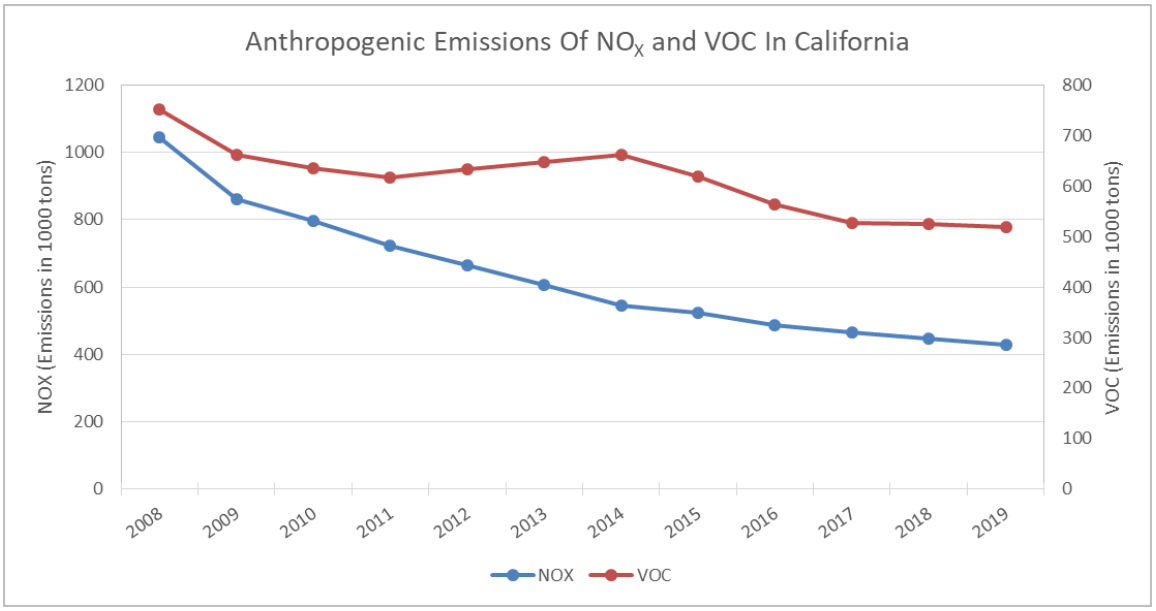

Source: https://www.epa.gov/air-emissions-inventories/air-pollutant-emissions-trends-data (under *State Annual Emissions Trend*).

Figure 2-7. Anthropogenic Emission Trends of NO_X and VOC in California, 2008–2019.

Figure 2-8 shows a downward trend in NO_x emissions and a slight increase in VOC anthropogenic emissions in Clark County from 2008–2017.

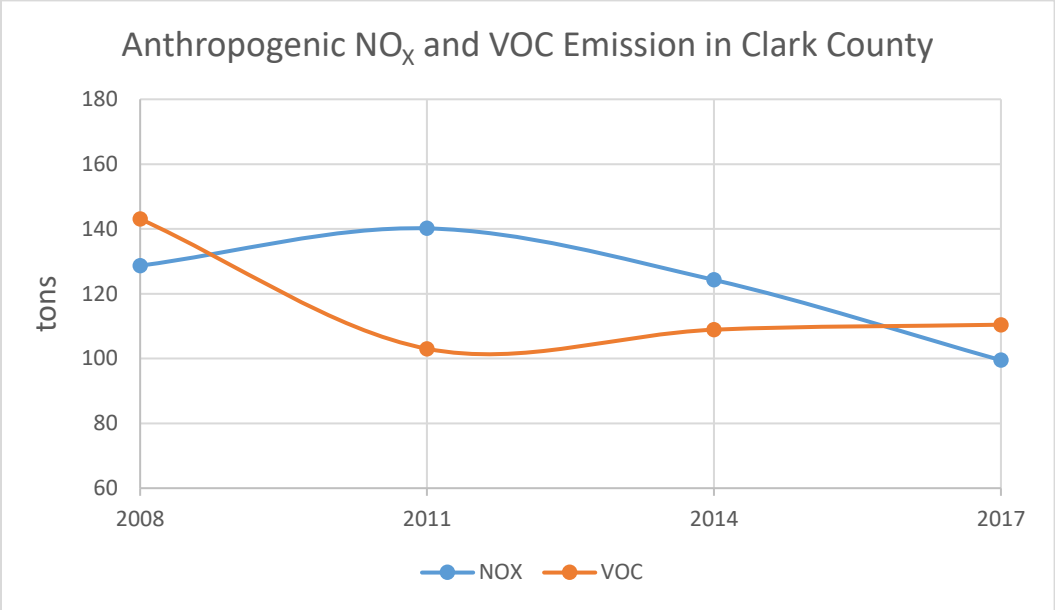

Source: https://www.epa.gov/air-emissions-inventories/national-emissions-inventory-nei.

Figure 2-8. Anthropogenic Emission Trends of NO_x and VOCs in Clark County, 2008–2017.

After a substantial reduction in NO_x emissions (approximately 55% in California and 25% locally) over the past 10 years, Figure 2-9 illustrates how the eight-hour ozone 4th highest averages in Clark County generally trended downward from 2009–2019 (except in 2018).

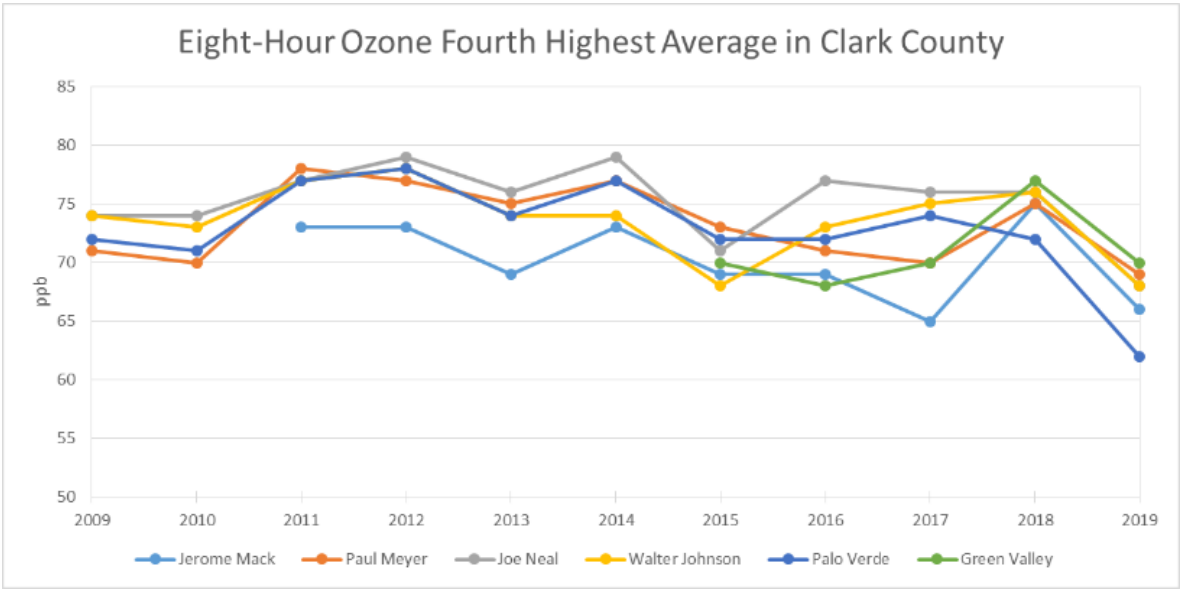

Figure 2-9. Eight-hour Ozone 4th highest Average at Monitors in Clark County, 2009–2019.

2.2.2 Weather Patterns Leading to Ozone Formation

Most of the high ozone days in the Las Vegas Valley occur from May through August. During these months, warmer temperatures lead to the development of regional-scale southwest-north-east plains-mountain circulations and locally-driven valley and slope flows (Stewart et al. 2002). In general, winds during the nocturnal regime are dominated by downslope flows from the east and southwest converging into Las Vegas; downslope flows have also been observed northeast of the Spring Mountain Range. Southeasterly to southerly wind flow develops during the morning transition period, but the winds shift to the southwest by mid-afternoon as the mixed layer grows in depth and plains-mountain winds develop, driven by the thermal contrast between the land and the Gulf of California. This regional-scale flow converges with southeasterly up-valley flow in the LVV, and these winds typically persist until well into the night, when the nocturnal regime prevails again.

The convergence of afternoon southwesterly plain-mountain and southeasterly up-valley flows at the northwestern terminus of the valley frequently results in elevated ozone levels at JO and WJ. Figure 2-10 illustrates the typical ozone season (May–August) diurnal ozone patterns at the 50th and 95th percentiles at all monitors in HA 212. These patterns are based on historic ozone data from 2014–2018.

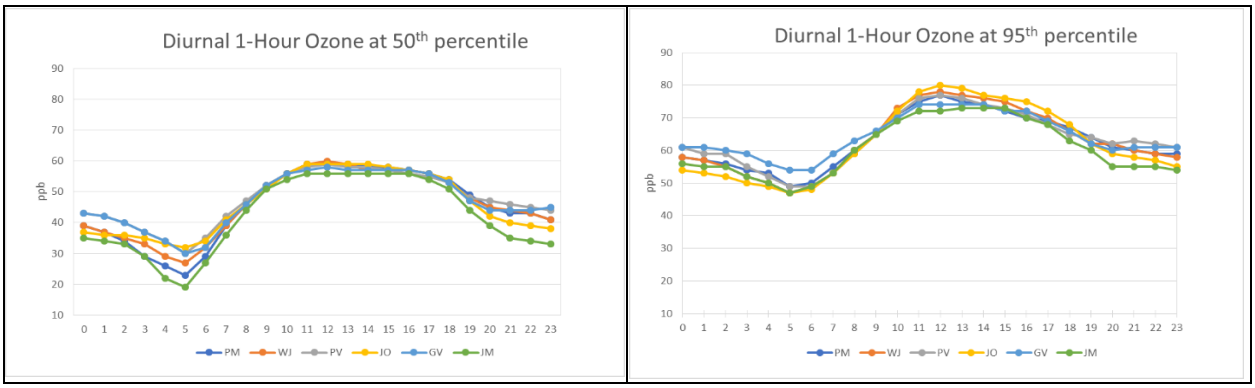

Figure 2-10. Typical Ozone Season 1-Hour Ozone Diurnal Pattern for 50th and 95th Percentile Values at Clark County Monitors.

2.2.3 Weekday and Weekend Effect

Figure 2-11 depicts air quality monitors in the LVV; the NO_2 monitors at Rancho Teddy (RT), Casino Center (CC), Sunrise Acres (SA), JM, and JO are marked as red dots. Most anthropogenic precursors are emitted from the urban core and follow a diurnal pattern related to traffic patterns, which peak twice daily at the morning and evening rush hours (Figure 2-12).

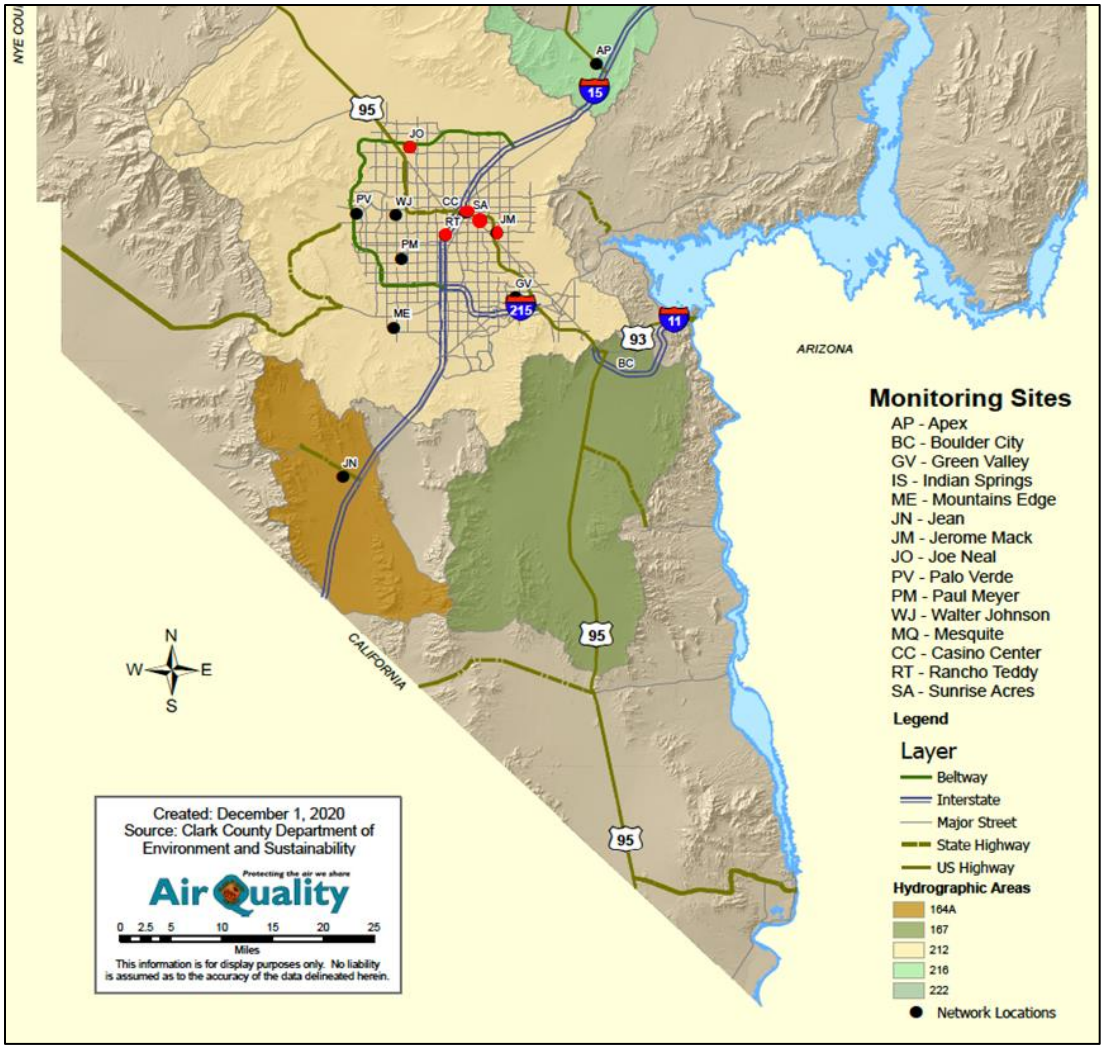

Note: Red dots = NO_2 monitors.

Figure 2-11. Locations of NO_2 Monitors.

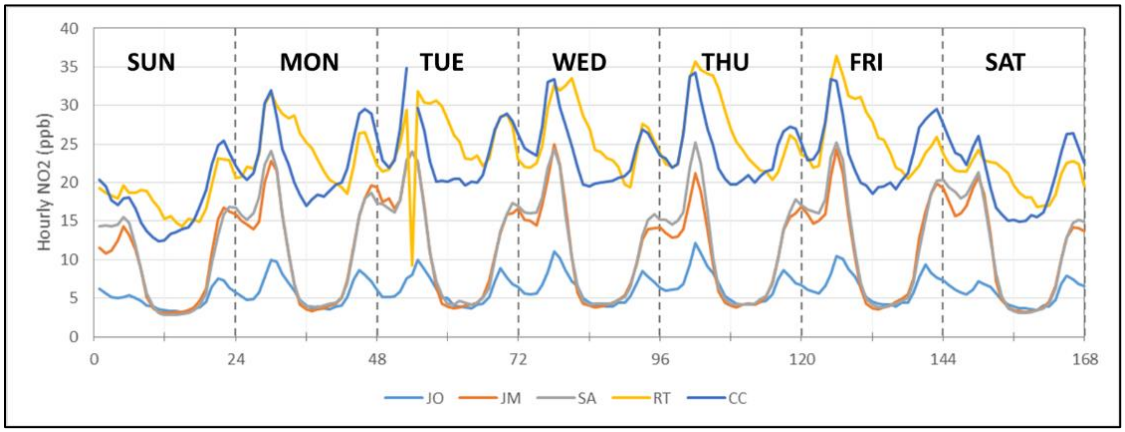

Figure 2-12. Weekly Pattern for 1-Hour NO_2 at Monitors, 2014–2019 (May-August).

Figure 2-13 shows that daily average NO_2 concentrations are lower on weekends than weekdays. The highest NO_2 concentrations are at RT and CC (urban core-downtown), and the lowest are at JO (further downwind). These weekly patterns are based on historic hourly and daily NO_2 concentrations recorded between 2014 and 2019 (May–August).

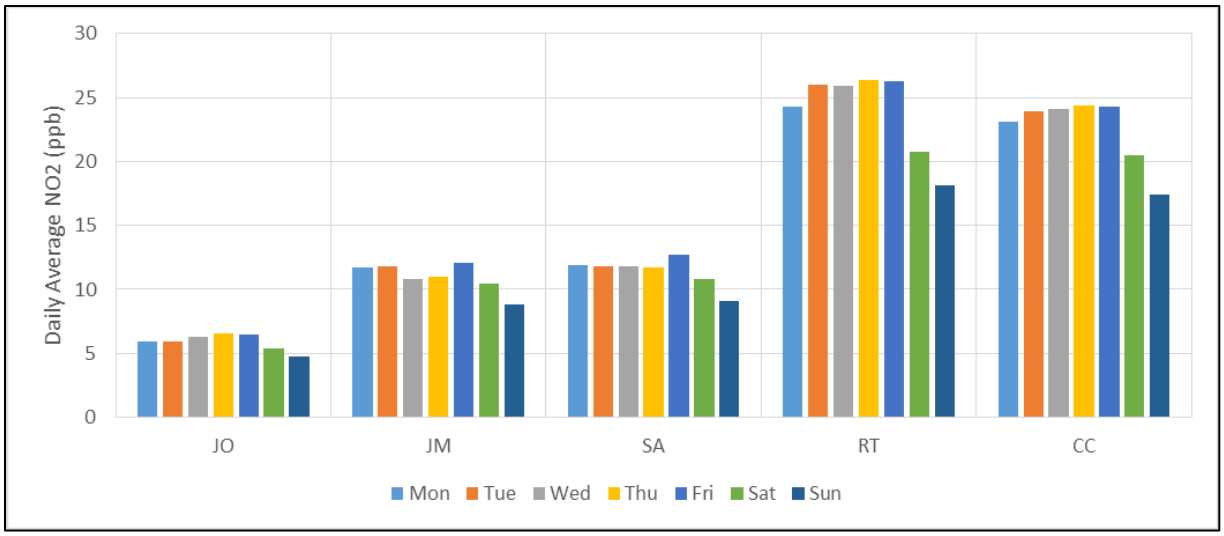

Figure 2-13. Weekly Pattern for 24-Hour NO_2 Average at Monitors, 2014–2019 (May–August).

Figure 2-14 shows the mean MDA8 O_3 at six monitors in HA 212 (see Figure 2-2) and the upwind monitor at Jean. It shows these sites have a similar weekly pattern, with the highest MDA8 O_3 on Fridays and Saturdays despite significantly lower concentrations of NO_2 (an O_3 precursor) on Saturdays (Figure 2-13). It also indicates MDA8 O_3 at those sites differs minimally between weekdays and weekends, with a maximum difference of 1.7~2.4 ppb. The data in this analysis are based on historic O_3 concentrations recorded between 2014 and 2019 (May–August).

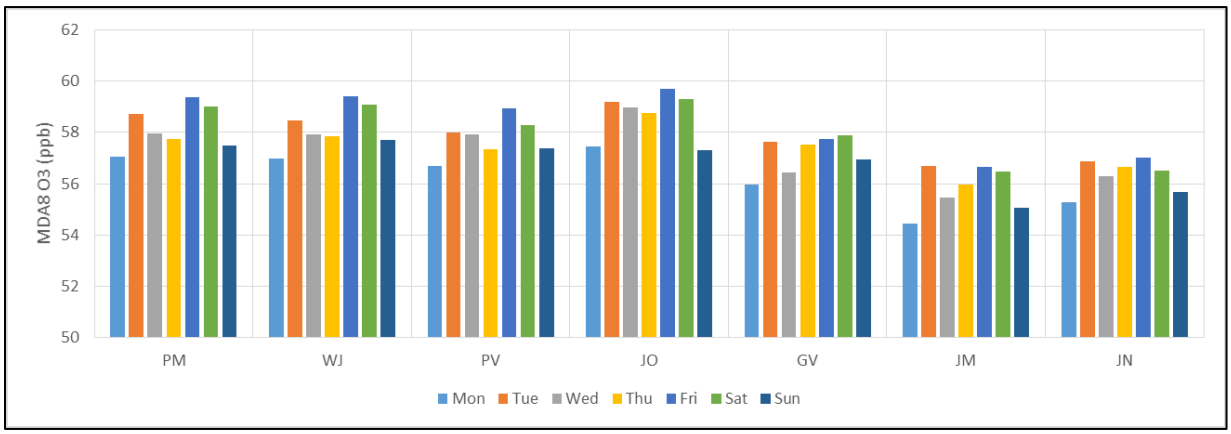

Figure 2-14. Weekly Pattern for MDA8 O_3 Average at Monitors, 2014–2019 (May–August).

3.0 EVENT SUMMARY AND CONCEPTUAL MODEL

3.1 PREVIOUS RESEARCH ON OZONE FORMATION AND SMOKE IMPACTS

The impact of wildfires on ozone concentrations at both local and regional levels has been studied extensively. Nikolov (2008) provides an excellent summary of past studies, as well as a conceptual discussion of the physical and chemical mechanisms contributing to observed impacts. Nikolov concludes that on a regional scale, biomass burning can significantly increase background surface ozone concentrations, resulting in NAAQS exceedances. Pfister et al. (2008) simulated the large fires of 2007 in northern and southern California; the authors found ozone increases of approximately 15 ppb in many locations and concluded, "Our findings demonstrate a clear impact of wildfires on surface ozone nearby and potentially far downwind from the fire location, and show that intense wildfire periods frequently can cause ozone levels to exceed current health standards." In a presentation at an emission inventory conference, Pace et al. (2007) modeled the June 2005 California fires, showing that the wildfire impacts added as much as 15 ppb to ozone concentrations in southern Nevada (Figure 3-1).

Finally, in one of DES's own studies (DES 2008), aircraft flights through smoke plumes demonstrated increased ozone concentrations of 15 to 30 ppb in California. Two other field campaign studies (DES 2013 & 2017) conducted by National Oceanic and Atmospheric Administration (NOAA) scientists have shown that large fires in California could have adversely impacted the air quality in Clark County.

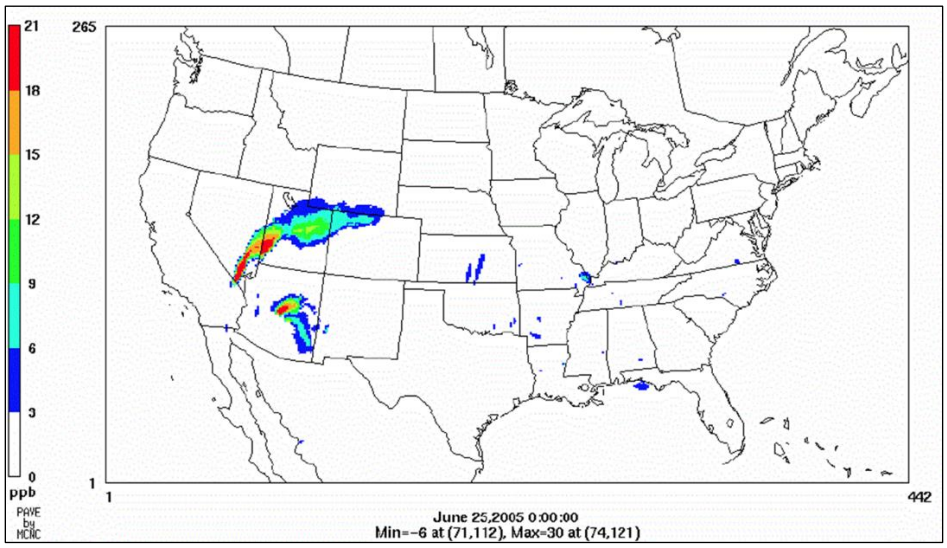

Figure 3-1. Difference ("Fire" / "No Fire") in Maximum 8-hour Ozone for June 25, 2005.

3.2 CALIFORNIA WILDFIRES IN 2018

Wildfires in the western states are worsening every year: they are bigger, hotter, more deadly, and more destructive. In California in 2018, the combination of natural fuel from a record 129 million trees killed by drought and bark beetles (as reported by the United States Forest Service) and compounding atmospheric conditions led to numerous large and small wildfires. The number

of fires and burned area increased greatly in June and July, as shown in Figure 3-2. Significant wildfires started breaking out in June of that year; later on in the summer, a series of large wildfires erupted across California, mostly in the northern part of the state, including the destructive Carr and Mendocino Complex Fires.

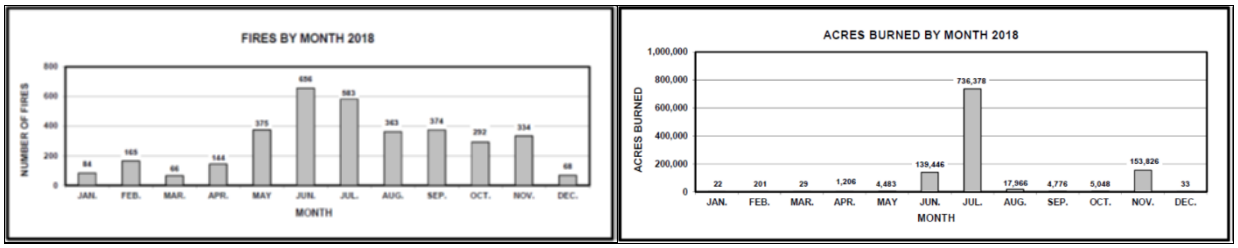

Source: CAL FIRE 2018 Wildfire Activity Statistics Report.

Figure 3-2. Number of Fires and Acres Burned by Month.

Figure 3-3 shows the more frequent ozone exceedances in the LVV after mid-June, reflecting the impact of the California wildfires during this period.

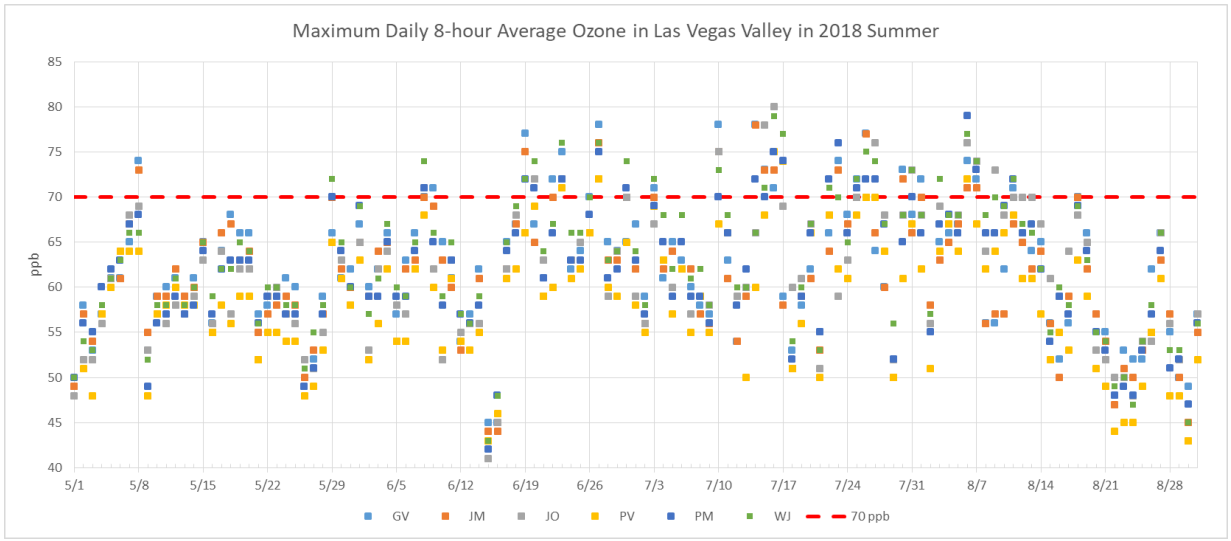

Figure 3-3. MDA8 Ozone Levels at LVV Monitors during 2018 Ozone Season.

3.3 AUGUST 6–7, 2018

By early August, smoke from many California wildfires was flowing into southern Nevada, but especially from the two biggest: the Mendocino Complex and Carr fires. Other large fires began re-burning intensively during this time, including Ferguson and Lions: by August 6, these two fires had grown to nearly 100,000 acres combined. A new fire ignited on August 1 near the Donnell Reservoir in the Stanislaus National Forest; it had burned 13,814 acres by August 8, when it was only 5% contained. Figure 3-4 shows these fire locations and the smoke plumes from northern/central California being transported towards the southern California desert and southern Nevada on August 5.

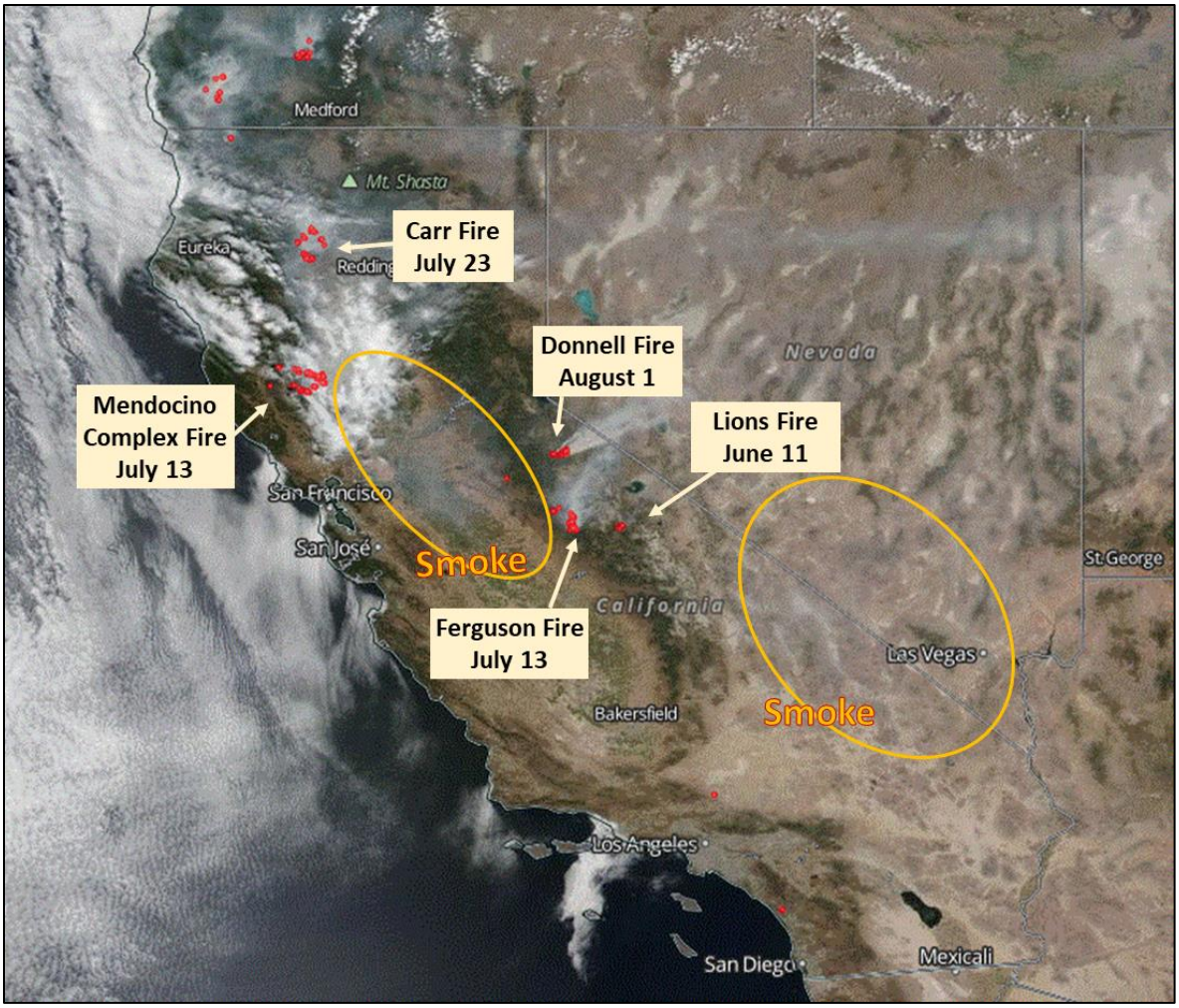

Source: NASA Worldview.

Figure 3-4. Fire Locations on August 5.

The 500-mb upper air analysis for August 4–7 in Figure 3-5 shows the western U.S. under the influence of a broad, flat ridge that dominated from the West Coast to Texas, with a low pressure system in the Gulf of Alaska. This low pressure system produced an upper level disturbance on August 4, located just offshore of the northwestern U.S. and depicted as a black, curved, dashed line in the 500-mb upper air analysis. On August 5, that upper level disturbance moved east towards Idaho, extending south into northern Nevada. It continued moving east through August 7.

As the upper level disturbance moved through the northwestern U.S., a strong ridge built up behind the exiting disturbance. In the atmosphere's lower boundary layer, just above the surface at the 850-mb level (Figure 3-6), a thermal low was in/near southwestern Nevada on August 4–6. This feature provided some regional dispersion; the winds generally were northwesterly from northern California to central/southern California, and transitioned to southwesterly toward the LVV. On August 6-7, the warmer temperature area on the 850-mb maps was over Clark County; the skew-T diagrams in Figure 3-7 show that both days had a deep and neutrally nocturnal residual layer. They indicate that substantial stability and capping (i.e., temperature inversion) was occurring in the LVV on those days.

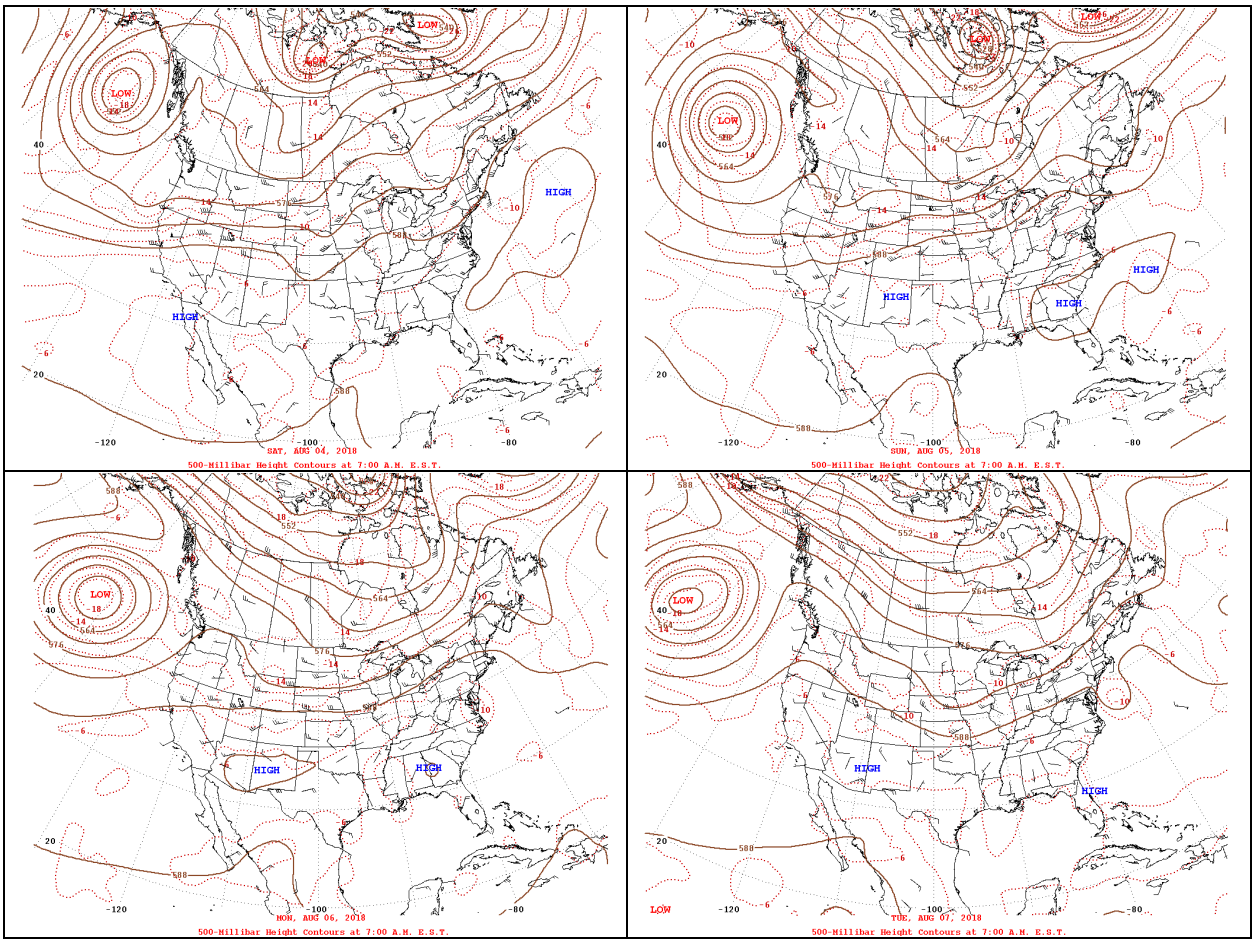

Figure 3-5. 500-mb Weather Patterns at 7 AM EST, August 4–7.

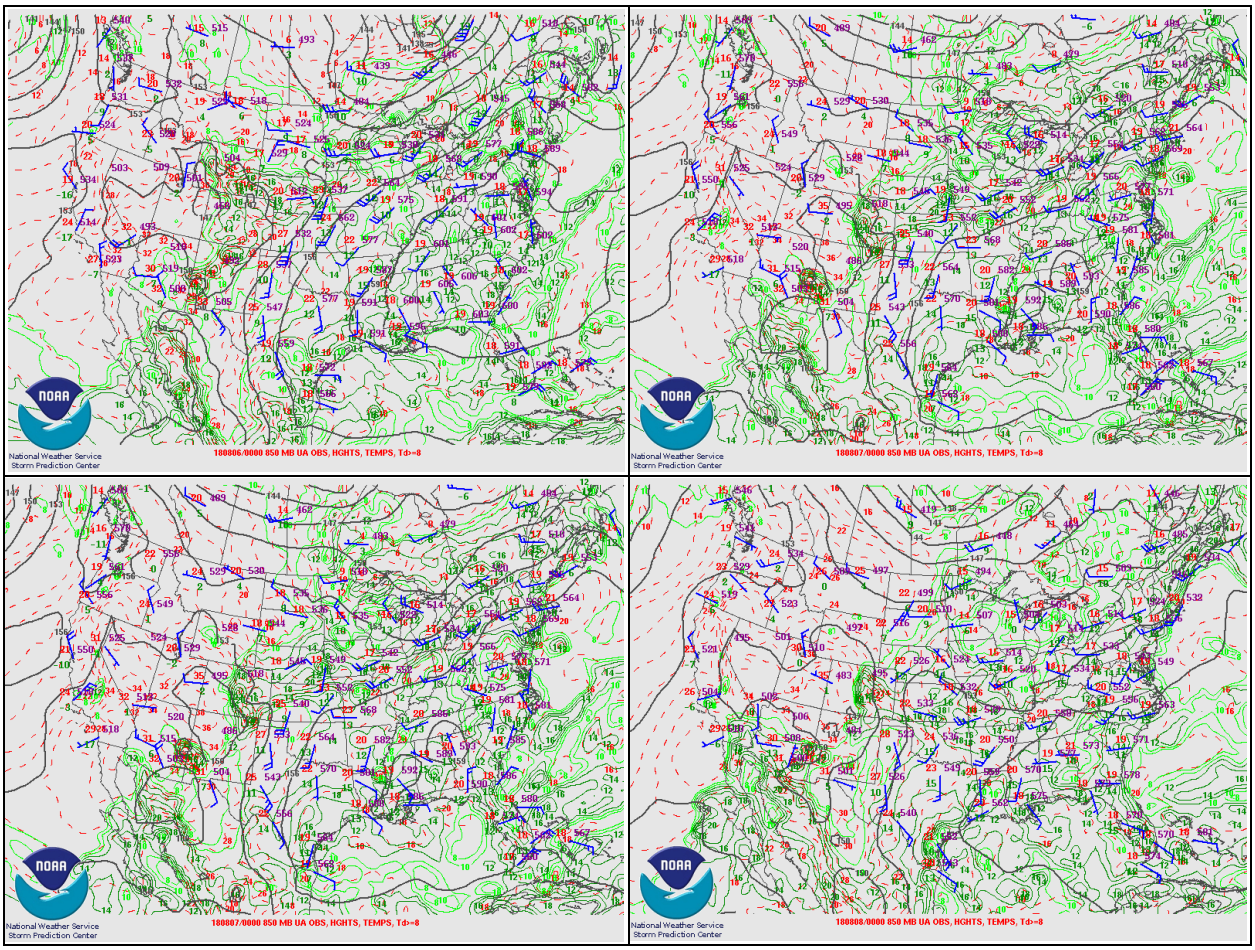

Figure 3-6. 850-mb Constant Pressure Map for 4 AM PST, August 4–7.

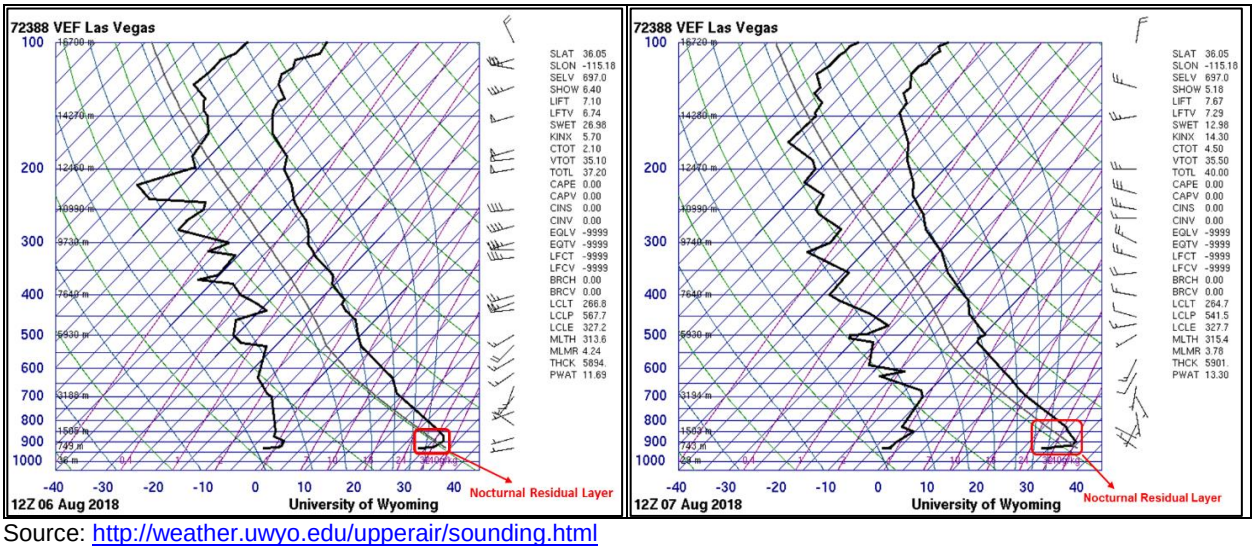

Source: http://weather.uwyo.edu/upperair/sounding.html

Figure 3-7. Upper LVV Weather: Skew-T diagrams at 12Z on August 6–7.

The surface analysis maps for August 4–7 in Figure 3-8 show generally how a high pressure system, associated with light and variable winds, dominated the LVV and a strong southwest trough was moving over Oregon and northern California toward southern California and Nevada. A stationary front hovered over southern Nevada on August 5–6 before moving east and transitioning to a cold front. Behind the stationary/cold front, the smoke subsided to the surface and merged with smoke from other wildfires in California under the high pressure system dominating the southwestern U.S. They contributed to ozone exceedances at all monitors (71~79 ppb, Table 1-1) in HA 212 on August 6. Figure 3-9 illustrates a simplified conceptual model of the August 6–7, 2018, wildfire-influenced ozone event.

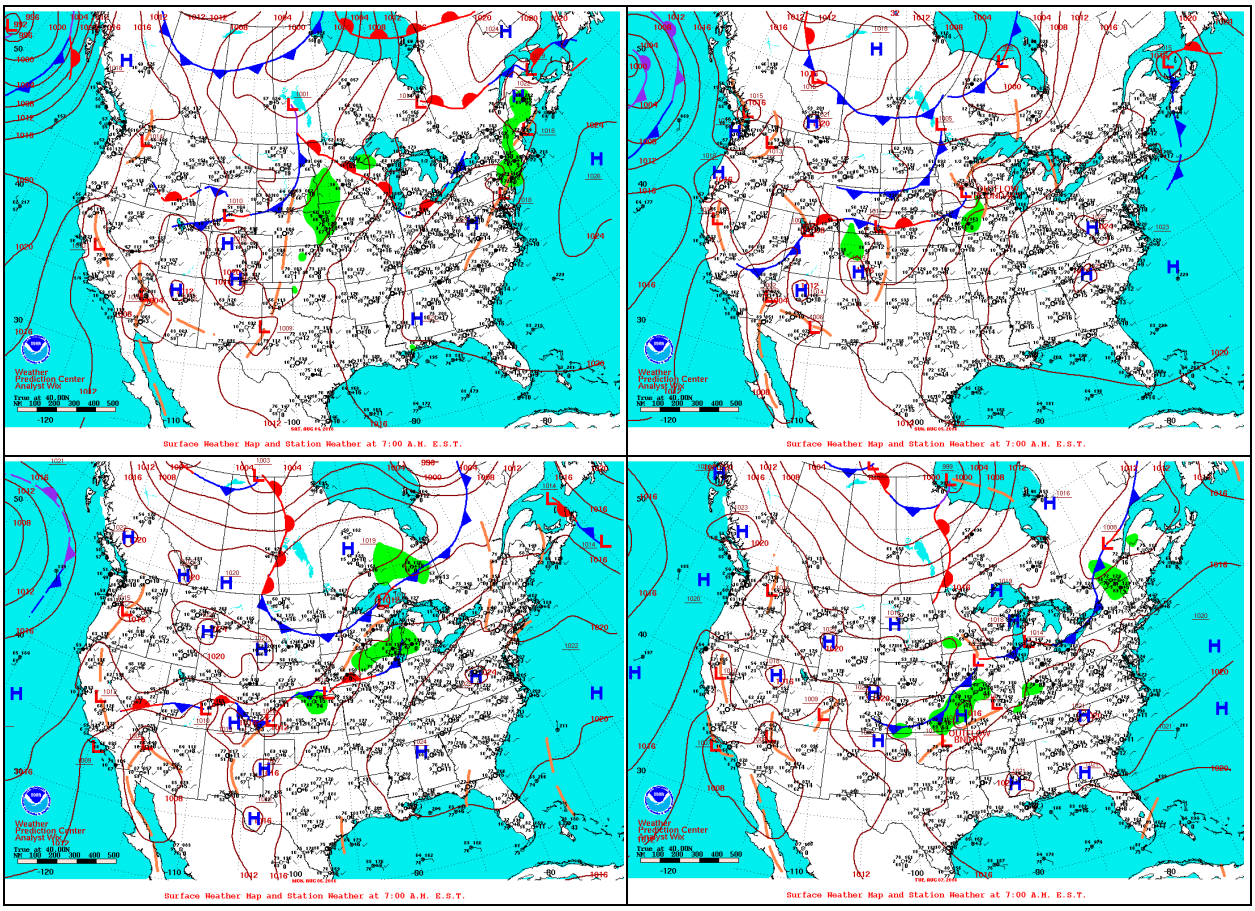

Figure 3-8. Surface Analysis for 4 AM PST, August 4–7, 2018.

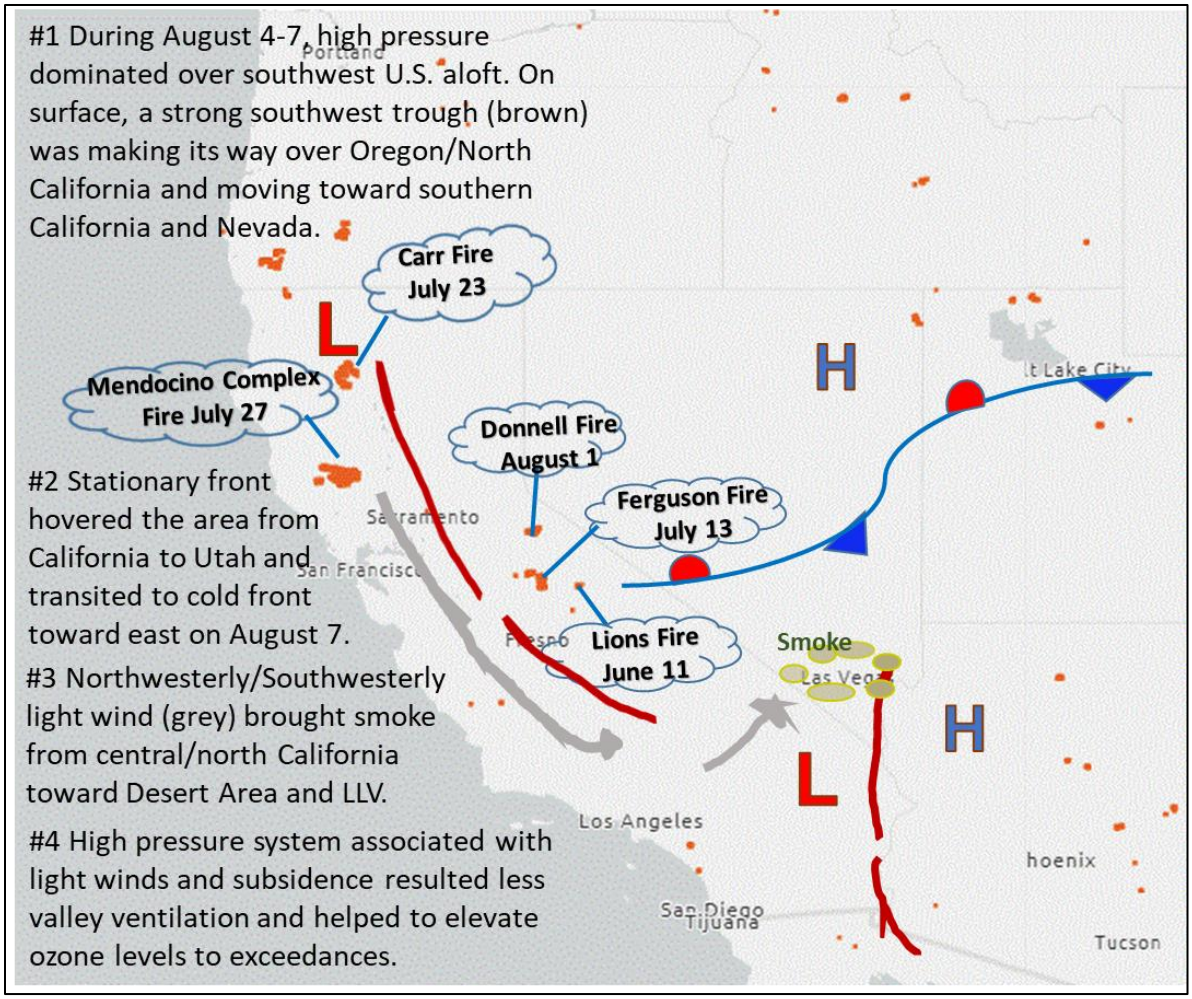

Figure 3-9. Simple Conceptual Model of August 6–7 Wildfire-Influenced Ozone Event.

4.0 CLEAR CAUSAL RELATIONSHIP

4.1 ANALYSIS APPROACH

Based on EPA's exceptional event guidance, this package provides Tier 1, Tier 2, and Tier 3 analyses to demonstrate a clear causal relationship between the wildfire event and monitored ozone exceedances. The demonstrations in this section provide (1) a comparison of the ozone data requested for exclusion against historical ozone concentrations at the monitor, and (2) a presentation of the path along which fire emissions were transported to the affected monitors.

Tier 1 Analyses

- Event day ozone concentrations are 5–10 ppb higher than non-event-related concentrations (95th percentiles for hourly seasonal ozone for 2014–2018).

Tier 2 Analyses

- Key Factor #1: Q/d Analysis.
- Key Factor #2: Comparison of the event-related MDA8 ozone with historical non-event-related high ozone concentrations (>99th percentile from 2014 to 2018 of MDA8 ozone, or the top four highest daily ozone measurements).
- Visible satellite imagery.
- Hazard Mapping System (HMS) smoke map.
- Ground visibility imagery.
- Hybrid Single-Particle Lagrangian Integrated Trajectory (HYSPLIT) model backward trajectories.
- Cloud-Aerosol Lidar and Infrared Pathfinder Satellite Observation (CALIPSO) satellite retrieval: Vertical profile measurements of atmospheric aerosols.
- Concurrent rise in ozone concentrations.
- Analysis of PM2.5 speciation data.
- Analysis of levoglucosan (trace of fire emissions).
- Supporting ground measurements: Event-related diurnal PM2.5, NO2, and CO (wildfire plume components) concentrations showed elevated concentrations and/or changes in diurnal profile consistent with smoke impacts.

Tier 3 Analyses

- GAM statistical model.

Key Factor #1 for a Tier 2 analysis uses an **emissions divided by distance (Q/d)** relationship to estimate the influence of fire emissions on a downwind monitor. If Q/d • (daily aggregated fires) ≥ 100, then the fires satisfy the Q/d test.

We examined Aerosol Optical Depth (AOD) maps from the Moderate Resolution Imaging Spectroradiometer (MODIS) instruments onboard the National Aeronautics and Space Administration's (NASA's) Aqua and Terra satellites using the Worldview tool. Since AOD indicates the

concentration of aerosols in the total atmospheric column, analyzing AOD maps can help to recognize the movements of smoke.

In addition to analysis of $PM_{2.5}$ speciation data, levoglucosan—a unique tracer for burning biomass in $PM_{2.5}$ samples—can serve as a wildfire indicator. Levoglucosan has an atmospheric lifetime of one to four days before it is lost due to atmospheric oxidation, and can therefore be used as a tracer of biomass burning (wildfires) far downwind from its source (Hoffmann et al. 2009; Hennigan et al. 2010; Bhattarai et al. 2019; Lai et al. 2014). During the summer of 2018, DES collected $PM_{2.5}$ samples every three days at the Jerome Mack and Sunrise Acres monitoring stations. Sample analysis—including for levoglucosan, a wildfire marker—was done by the Desert Research Institute (DRI).

A GAM is a type of statistical model that allows the user to predict a response based on the linear and non-linear effects of multiple variables (Wood 2017). A GAM model developed by Sonoma Technology was used to describe the relationship between MDA8 levels of ozone and primary predictors (e.g., prior day's ozone, meteorology, and transport) from 2014–2020. The details for the model's construction and verification are described in Section 3.3.3, "GAM Statistical Modeling," of *Exceptional Event Demonstration for Ozone Exceedances in Clark County, Nevada—June 22, 2020*. By comparing GAM-predicted ozone values with actual measured ozone concentrations (i.e., residuals), we can determine the effect of outside influences (e.g., wildfires or stratospheric intrusions) on ozone concentrations each day (Jaffe et al. 2004). The GAM model results presented in this document contain MDA8 ozone predictions, residuals, positive 95th percentile values, predicted fire influence, and percentile rank of positive residuals based on EPA guidance (EPA 2016), which were used to estimate wildfire influence under the meteorological conditions recorded at exceeding sites.

4.2 COMPARISON OF EVENT-RELATED CONCENTRATIONS WITH HISTORICAL CONCENTRATIONS

Outside of the transport of ozone and its precursors from California wildfires, elevated ozone levels in the LVV correlate to local weather conditions and home-grown (Figure 2-7) and upwind (Figure 2-8) California emissions. The declining ozone trend in the LVV (Figure 2-9) reflects the reduction of these emissions over the years. However, 2018 was an exceptional year, with more ozone exceedances than any of the prior years from 2014–2017 (Figure 1-1).

In general, warm, dry weather is more conducive to ozone formation than cool, wet weather. High winds tend to disperse pollutants and can dilute ozone concentrations. We examined three meteorological variables—daily maximum surface temperature, daily average wind speed, and daily average relative humidity—at McCarran International Airport during the 2014–2018 summer months to depict the year-to-year variation of local weather conditions (Figure 4-1).

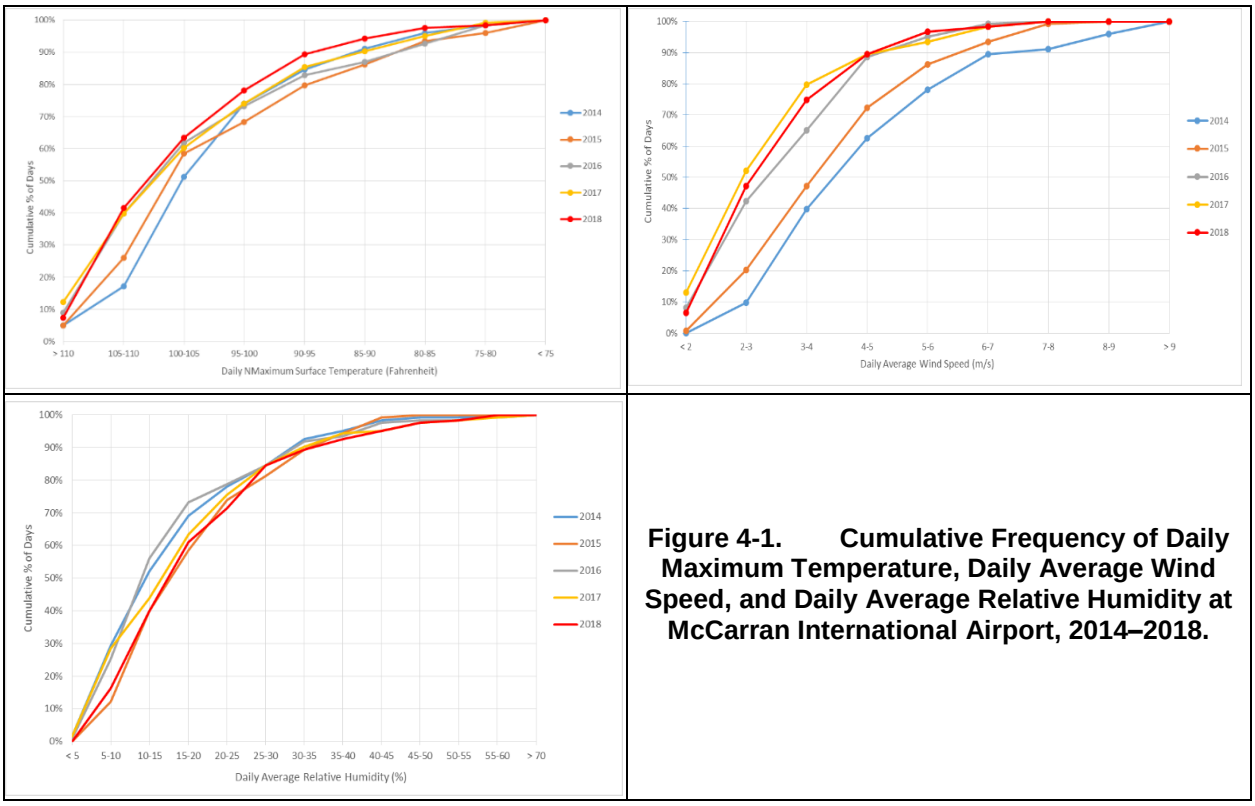

Figure 4-1. Cumulative Frequency of Daily Maximum Temperature, Daily Average Wind Speed, and Daily Average Relative Humidity at McCarran International Airport, 2014–2018.

Overall, 2018 had lower wind speeds, slightly higher temperatures, and slightly more moisture compared to previous years. Yet the mean of the 2018 MDA8 ozone is between 4.4 and 7.2 ppb higher than other years (Figure 4-2). Compared to 2014–2017, the summer of 2018 had more California wildfires (Figure 1-1) and relatively stagnant weather conditions (Figure 4-1). This increased background ozone levels in the LVV (Figure 4-2), resulting in a higher number of ozone exceedances than in previous years.

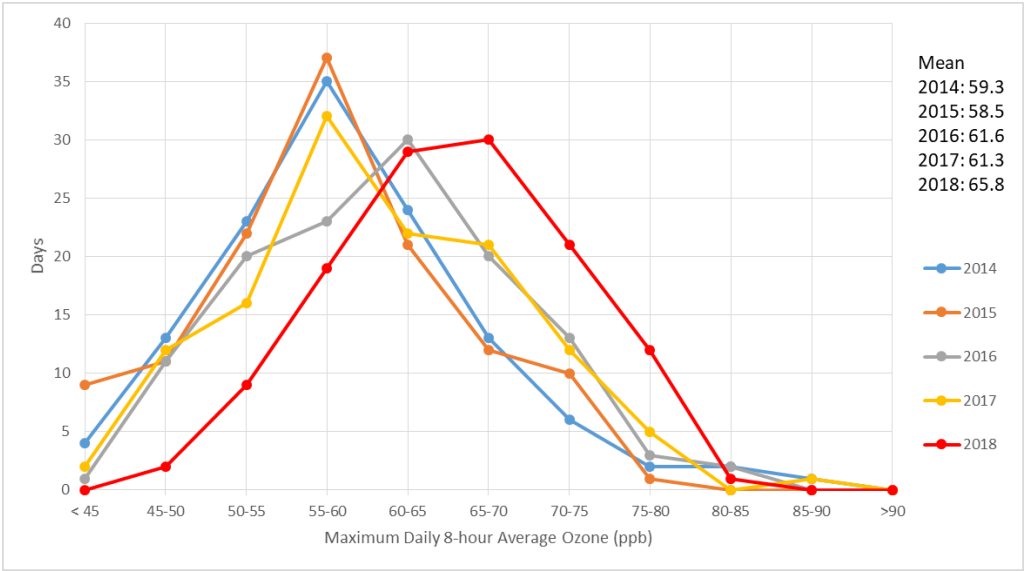

Figure 4-2. Distribution of Days by MDA8 Ozone Levels, 2014–2018.

Figures 4-3 through 4-8 show MDA8 ozone during the 2014–2018 ozone seasons plotted for each monitor against that monitor's multiseason 95th and 99th percentiles. Red circles indicate the ozone exceedances submitted for the 2018 exceptional events demonstration. All but the following sites and dates exceeded the 95th percentile: Walter Johnson on June 19 and July 15; Palo Verde on July 26 and 27; and Joe Neal on June 20, 23, and 27.

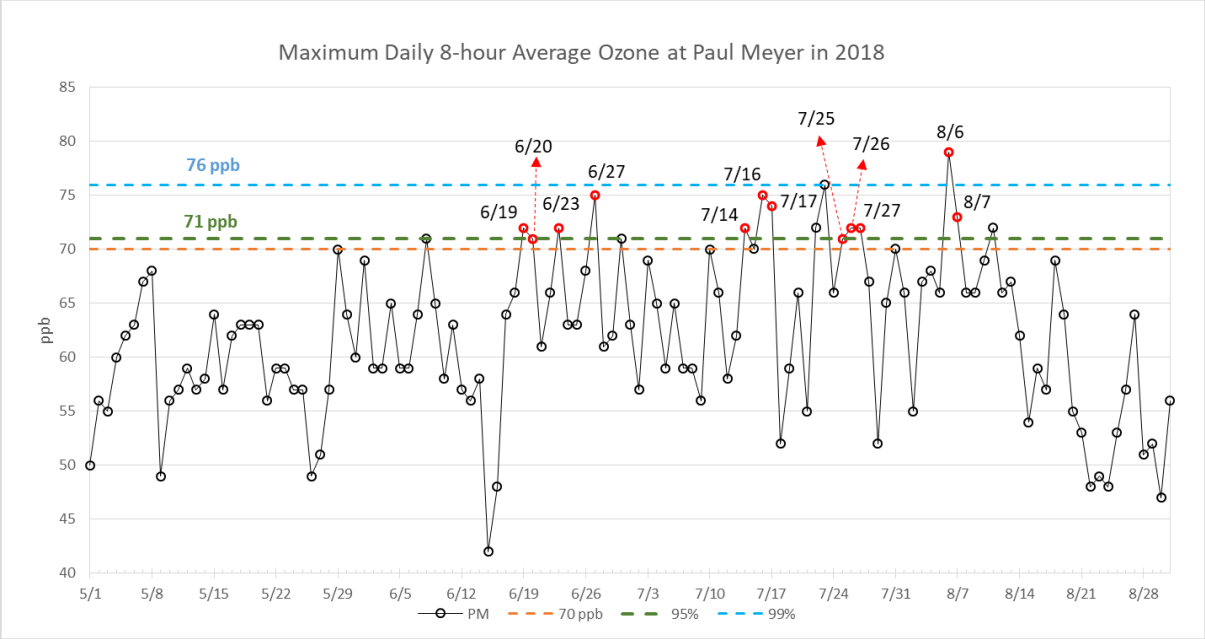

Figure 4-3. MDA8 Ozone at Paul Meyer, 2018 Ozone Season.

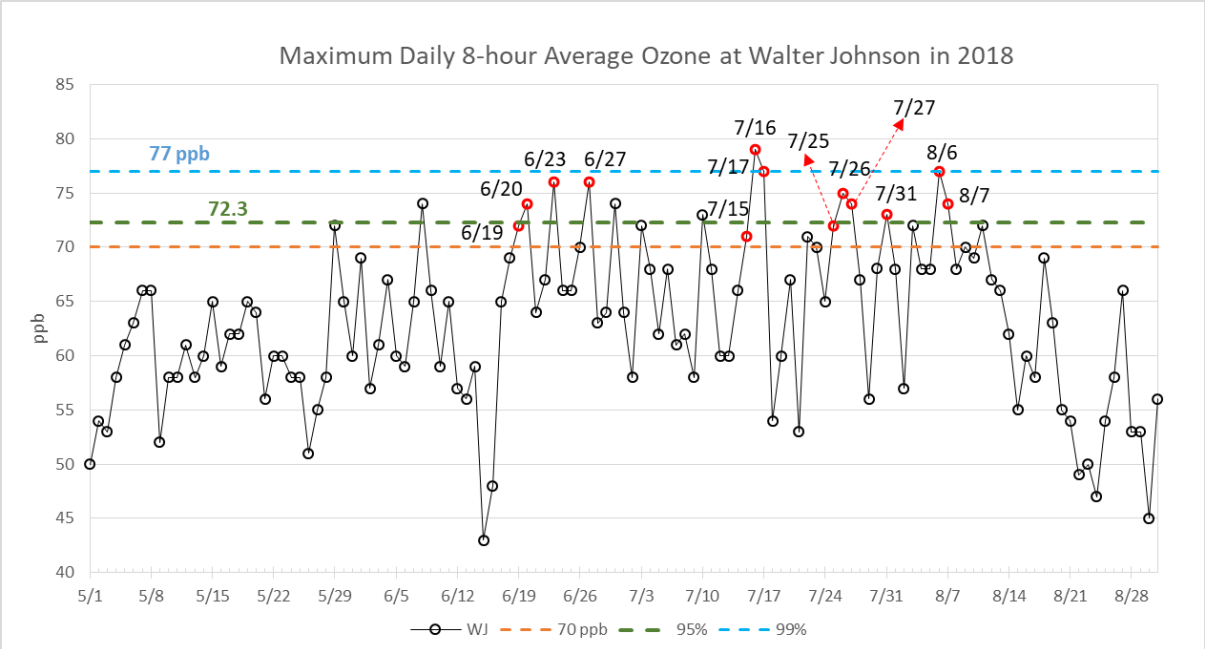

Figure 4-4. MDA8 Ozone at Walter Johnson, 2018 Ozone Season.

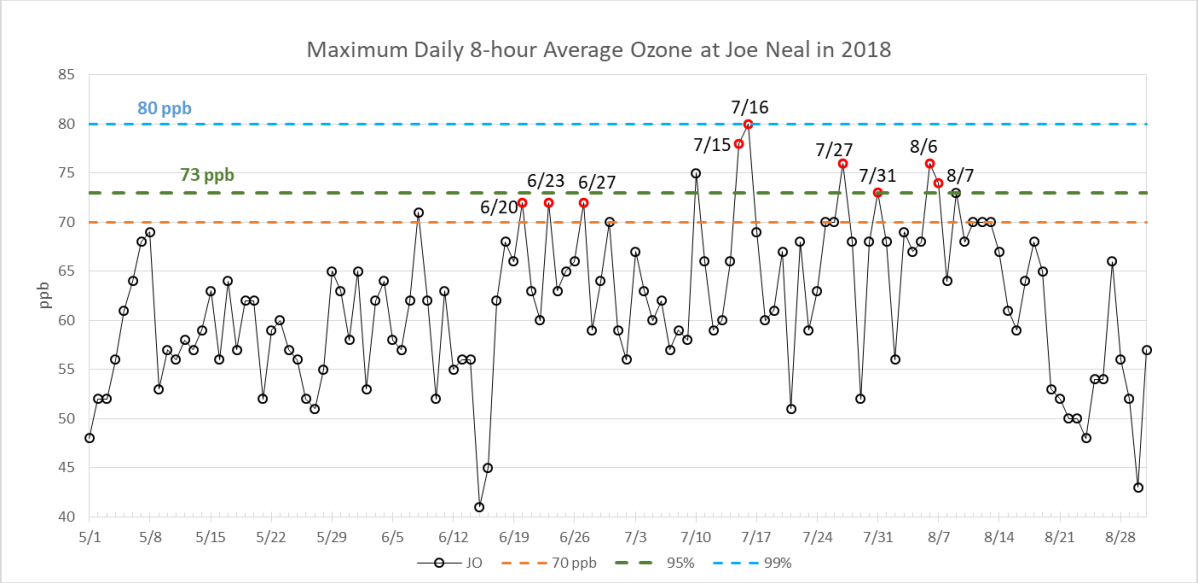

Figure 4-5. MDA8 Ozone at Joe Neal, 2018 Ozone Season.

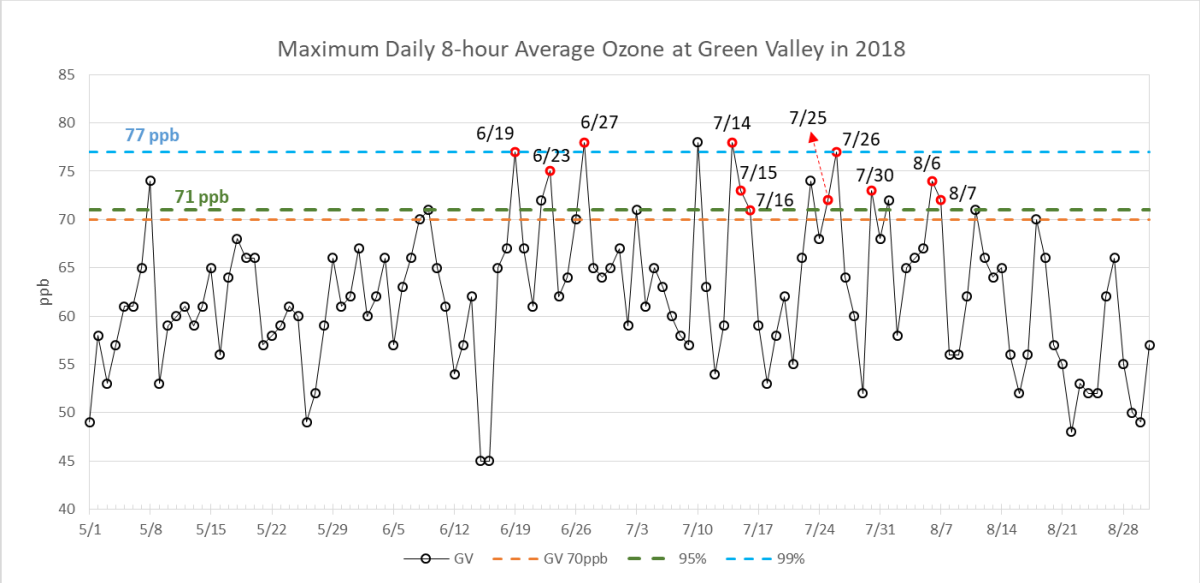

Figure 4-6. MDA8 Ozone at Green Valley, 2018 Ozone Season.

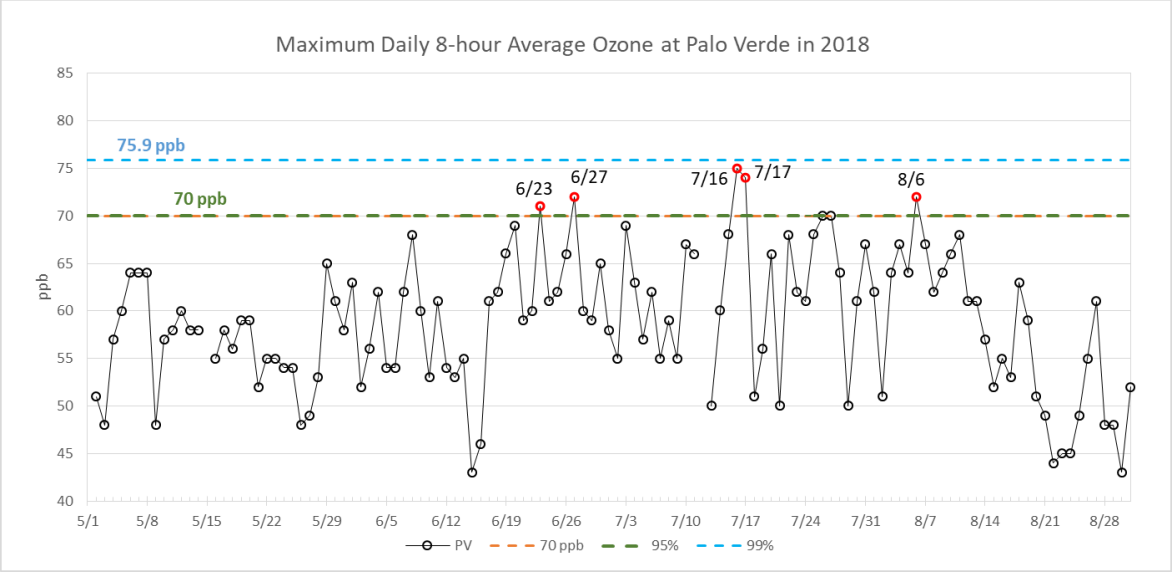

Figure 4-7. MDA8 Ozone at Palo Verde, 2018 Ozone Season.

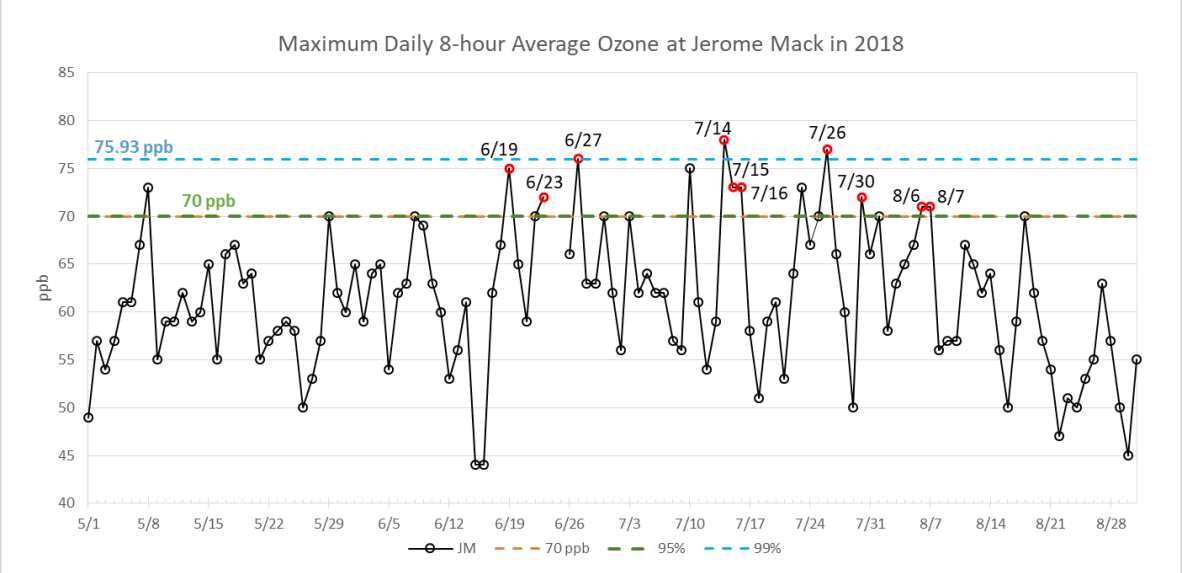

Figure 4-8. MDA8 Ozone at Jerome Mack, 2018 Ozone Season.

The ratio of $PM_{2.5}$ organic carbon (OC) to elemental carbon (EC) has been used to differentiate combustion sources of biomass burning and mobile sources, since biomass burning usually has a higher OC/EC ratio (ranging between 7 and 15) (Lee et al. 2005; Pio et al. 2008) than gasoline (ranging between 3.0 and 4.0) or diesel vehicles (<1.0) (Lee and Russell 2007; Zheng et al. 2007). The acquired $PM_{2.5}$ of OC and EC from EPA's Air Quality System (https://aqs.epa.gov/aqsweb/airdata/download_files.html) in the LVV is available only for Jerome Mack on a three-day sampling schedule.

Figure 4-9 shows the OC/EC ratio for May–August in 2018 and 2019 against the median OC/EC ratio of May–August (5.4, orange line) and September–April (3.4, green line) according to 2015–2017 and 2019 data. It clearly shows a larger wildfire influence in ozone season months than non-ozone season months, and more days impacted by wildfire during ozone season months in 2018 than 2019 (a clean year with the annual 4th highest MDA8 ozone for all monitors below the 2015 ozone NAAQS). Figure 4-10 shows a similar OC/EC ratio plot for an upwind monitor located at Rubidoux in the Riverside-San Bernardino, CA, area, with the median value of May–August (6.8, orange line) and September–April (3.4, green line). The larger summer median OC/EC ratio at Rubidoux makes sense, considering the difference in distance to the California fires. Comparing Figures 4-9 and 4-10 shows the daily variation in the OC/EC ratio at Jerome Mack generally follows the variation at Rubidoux, and that more days in 2018 than 2019 had an OC/EC ratio above the median value for both monitors. It strongly indicates Jerome Mack was frequently impacted by California wildfires in 2018.

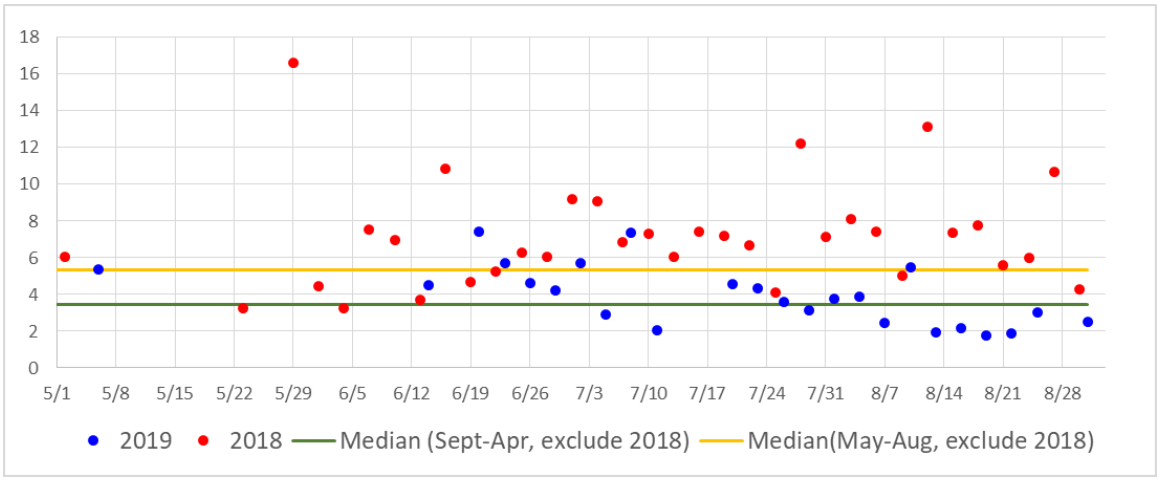

Figure 4-9. OC/EC ratio at Jerome Mack, 2018–2019 Ozone Season.

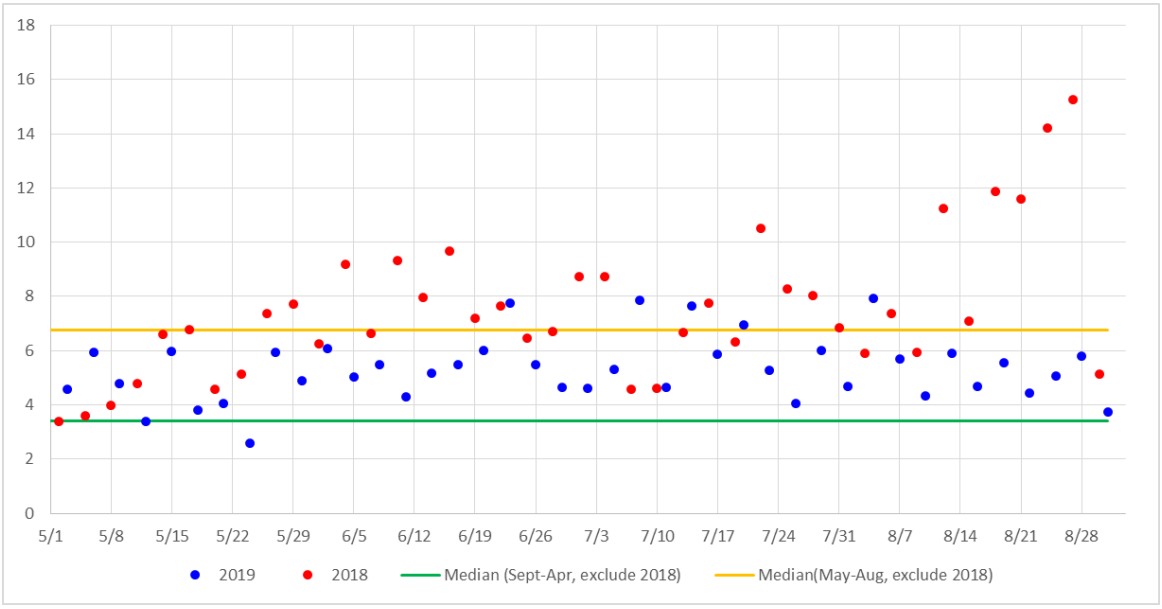

Figure 4-10. OC/EC ratio at Rubidoux, CA, 2018–2019 Ozone Season.

4.3 EVENT OF JUNE 27, 2018

4.3.1 Tier 1 Analysis: Historical Concentrations

Figures 4-11 and 4-12 show the hourly seasonal percentiles for ozone from 2014–2018 compared to measured hourly ozone on August 6-7, 2018, at exceeding sites. On August 6, the increases in O_3 at Green Valley, Walter Johnson, Paul Meyer, and Joe Neal were 12, 9, 4, and 11 ppb, respectively; on August 7, the increases in O_3 at Green Valley, Walter Johnson, Paul Meyer, and Joe Neal were 7, 8, 9, and 7 ppb, respectively. These data show the exceeding monitors on August 6–7 were 5–10 ppb higher (except Paul Meyer, which was 4 ppb higher on August 6) than non-event-related O_3 concentrations, and had a nontypical diurnal pattern. The data therefore provide strong evidence that wildfire emissions were transported to the location of the monitor.

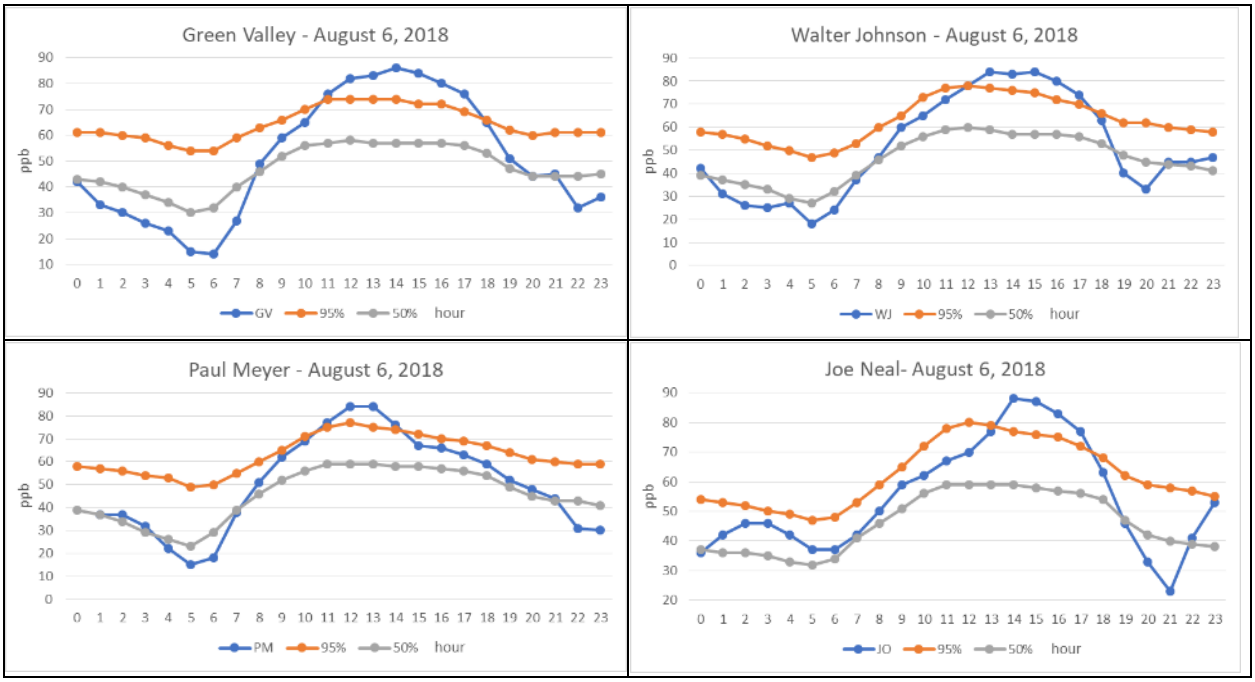

Figure 4-11. 5-Year Hourly Seasonal 95th & 50th Percentiles for O_3 and Observed O_3 on August 6.

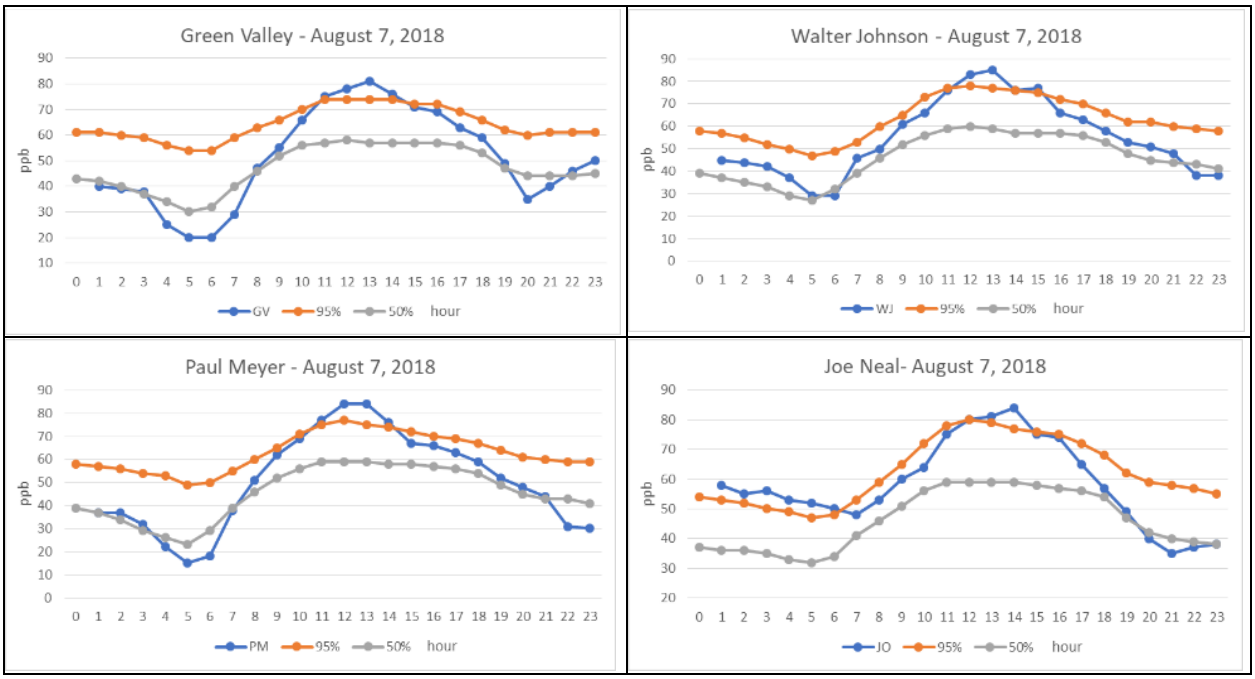

Figure 4-12. 5-Year Hourly Seasonal 95th & 50th Percentiles for O_3 and Observed O_3 on August 7.

4.3.2 Tier 2 Analysis

4.3.2.1 Key Factor #1: Q/d Analysis

Several large wildfires burning in California likely contributed to smoky conditions in the LVV on August 6–7. Figure 3-4 shows large fires burning in California on August 6. Table 4-1 provides the acreage burned as of August 7, based on available information. By determining which wildfires influenced the area's ozone concentrations, we can calculate the relationship between emissions and distance. This factor can then can be used to determine the influence of wildfire emissions on a downwind monitor.

Table 4-1. Data for California Fires Associated with August 6–7 Exceptional Event

Fire Name	Date Started	Date Contained	Cause	Acres Burned by Event Date[1]	Total Acres Burned
Lions	6/11/2018	10/1/2018	Lightning	7,889	13,347
Ferguson	7/13/2018	8/22/2018	Unknown	91,502	96,901
Carr	7/23/2018	8/30/2018	Vehicle	160,049	229,651
Mendocino Complex	7/27/2018	9/18/2018*	Human	290,692	459,123
Donnell	8/1/2018	10/31/2018	Unknown	12,000	36,450

[1]EE date = August 7, 2018.

The first key factor in a Tier 2 demonstration requires an analysis of wildfire smoke emissions and the distance from the fire to the affected monitor or monitors. The total daily emissions of NO_x and reactive VOCs (rVOCs) in tons is divided by the distance from the fire to the impacted monitors in km; the result, Q/d, is expressed in units of tons/km. EPA guidance states that an event may qualify for a Tier 2 demonstration if the Q/d value for a single fire, or the aggregate Q/d across multiple fires, exceeds a value of 100 tons/km.

To identify qualifying fires, we calculated 24-hour HYSPLIT model back trajectories from the affected monitors' locations, starting on each hour of both the day of the exceedance and the day prior. We then created a buffer of uncertainty around each trajectory equal to 25% of the distance traveled, based on the overall uncertainty reported for HYSPLIT modeling by Draxler (1991).

Figures 4-13 and 4-14 show these back trajectories and buffers of uncertainty. All fires falling within the uncertainty buffer of one or more trajectories were considered candidates for calculating Q/d; subsequent calculations were based on the four fires that fell within the uncertainty buffer (Lions, Ferguson, Donnell, and Mendocino Complex). The Carr Fire was not included because the 24-hour back trajectories used for these analyses did not reach it; however, transport from that fire may have occurred over a longer period of time.

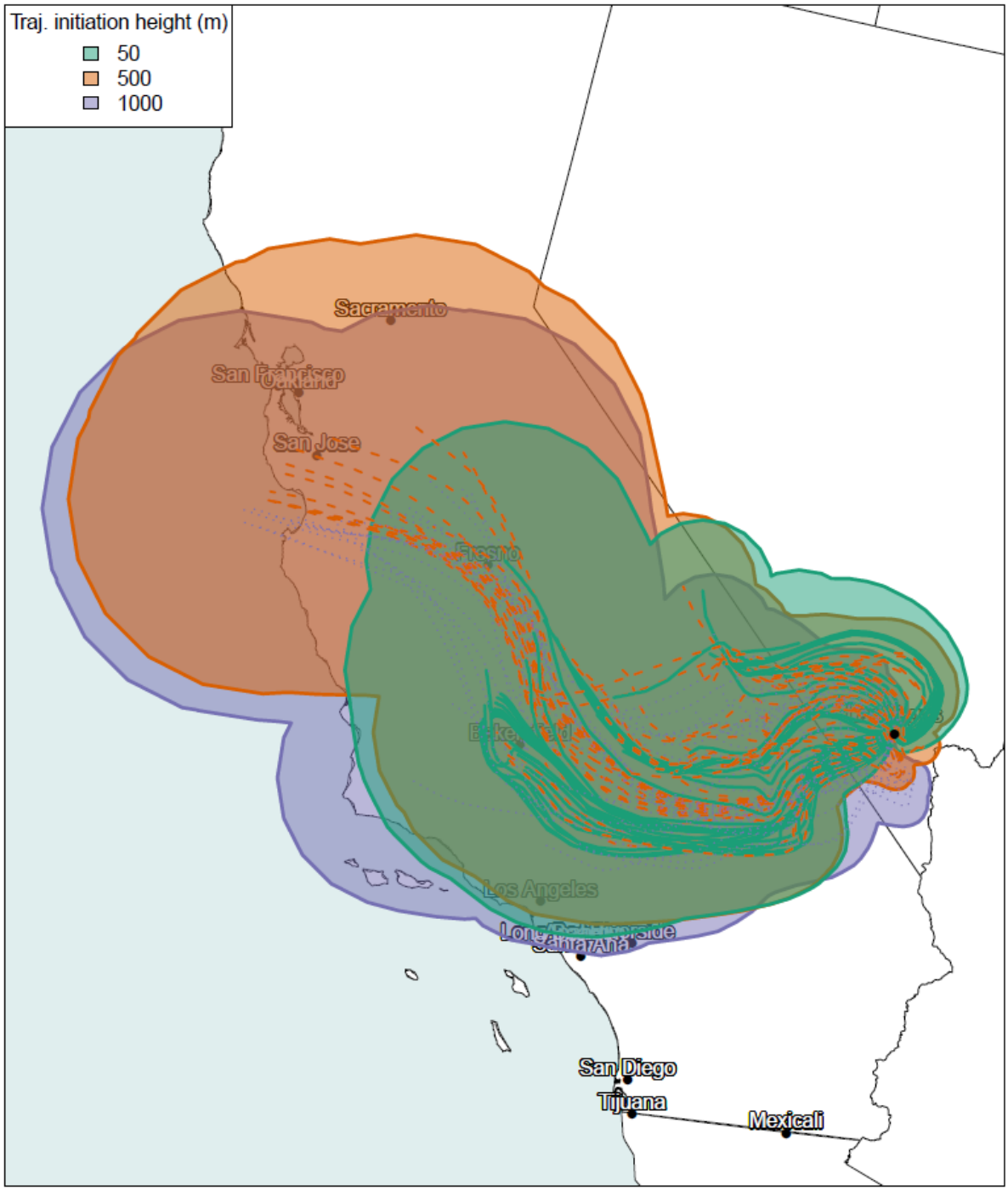

Note: Solid/dotted lines indicate 24-hour back trajectories colored polygons show uncertainty buffers. Fires within one or more uncertainty buffer(s) were considered candidates for calculation of individual or aggregate Q/d values.

Figure 4-13. Q/d Analysis for August 6.

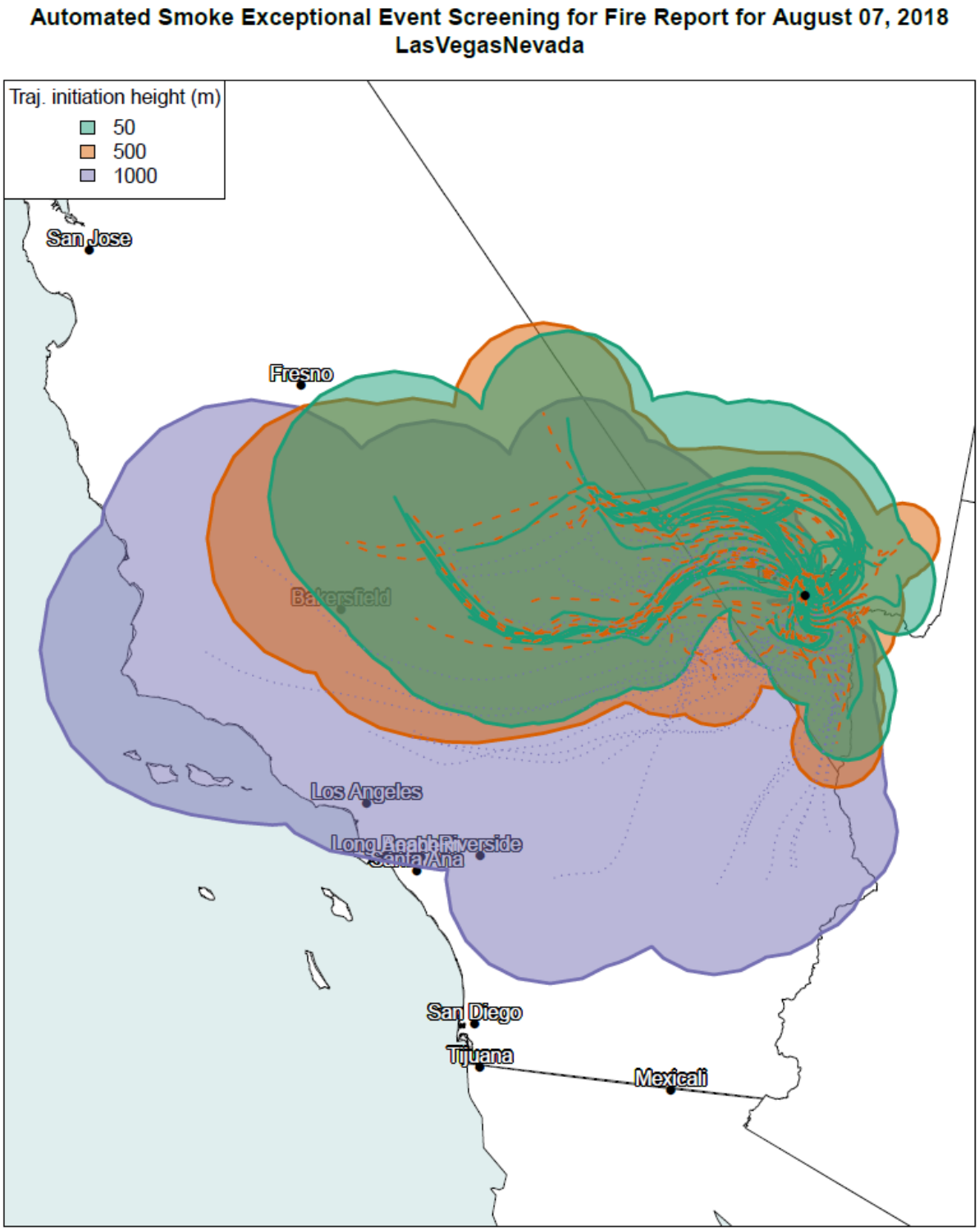

Note: Solid/dotted lines indicate 24-hour back trajectories colored polygons show uncertainty buffers. Fires within one or more uncertainty buffer(s) were considered candidates for calculation of individual or aggregate Q/d values.

Figure 4-14. Q/d Analysis for August 7.

BlueSky Playground version 3.0.1 (https://tools.airfire.org/playground/v3/) was used daily to estimate emissions of NO_x and VOCs for the Mendocino Complex, Lions, Ferguson, and Donnell fires on August 5–7 (Tables 4-2 through 4-4). Agency data and news reports were consulted to identify daily fire growth. Each fire's location was pinpointed to identify the distance to affected monitors and the fuel bed type. Emissions calculations were based on very dry conditions.

Daily Q/d results indicate that the identified fires produced significant emissions of NO_x and rVOCs during the days of the exceedance. Although emissions were not large enough to reach the Q/d threshold for a Tier 2 demonstration of 100 tons/km, these results suggest that smoke emissions from wildfires of a significant size did travel to the LVV and impact air quality.

Table 4-2. Daily Growth, Emissions, and Q/d for Fires on August 5, 2018

Fire Name	Area (acres)	Daily Growth (acres)	NO_x (tons)	VOCs (tons)	rVOCs (tons)	E (tons)[1]	Distance (km)	Q/d (tons/km)[2]	Fuel Loading
Lions[3]	7,889	340	15.15	553.51	332	347	385.0	0.9	Red fir forest
Ferguson[4]	91,502	1,869	42.13	315.75	189	232	450	0.5	CA live oak-blue oak woodland
Donnell[5]	11,074	5,260	234.45	8563.14	5,138	5,372	485	11.1	Red fir forest
Mendocino Complex[6]	273,664	18,682	383.08	12294.94	7,377	7,760	779.31	10.0	Jeffrey pine; ponderosa pine; Douglas fir; CA black oak forest

Note: Growth for all dates shown was obtained from agency estimates available from InciWeb or satellite estimates of growth.

[1] Sum of NO_x and rVOC emissions.
[2] Aggregate Q/d calculated for all fires shown is **21.1** tons/km.
[3] Source: https://web.archive.org/web/20181105223748/https://inciweb.nwcg.gov/incident/5850/.
[4] Source: http://thepinetree.net/new/?p=64963 and https://www.facebook.com/SierraNF/posts/ 2233518303585437.
[5] Source: https://www.modbee.com/news/article216154210.html and https://www.fs.usda.gov/detail/stanislaus/newsevents/?cid=FSEPRD590476.
[6] Source: https://web.archive.org/web/20190629195413/https://inciweb.nwcg.gov/incident/6073/.

Table 4-3. Daily Growth, Emissions, and Q/d for Fires on August 6, 2018

Fire Name	Area (acres)	Daily Growth (acres)	NO_x (tons)	VOCs (tons)	rVOCs (tons)	E (tons)[1]	Distance (km)	Q/d (tons/km)[2]	Fuel Loading
Lions[3]	8,138	249	11.1	405.37	243	254	385.0	0.7	Red fir forest
Ferguson[4]	93,331	1,829	41.23	308.99	185	227	450	0.5	CA live oak-blue oak woodland
Donnell[5]	11,344	270	12.03	439.55	264	276	485	0.6	Red fir forest
Mendocino Complex[6]	290,692	17,028	349.16	11206.42	6,724	7,073	779.31	9.1	Jeffrey pine; ponderosa pine; Douglas fir; CA black oak forest

Note: Growth for all dates shown was obtained from agency estimates available from InciWeb or satellite estimates of growth.

[1] Sum of NO_x and rVOC emissions.
[2] Aggregate Q/d calculated for all fires shown is **10.5** tons/km.
[3] Source: https://web.archive.org/web/20181105223748/https://inciweb.nwcg.gov/incident/5850/.
[4] Source: https://www.fresnobee.com/news/local/article216226095.html.
[5] Source: https://www.fs.usda.gov/detail/stanislaus/news-events/?cid=FSEPRD591422.
[6] Source: https://web.archive.org/web/20180809074721/https://inciweb.nwcg.gov/incident/news/6073.

Table 4-4. Daily Growth, Emissions, and Q/d for Fires on August 7, 2018

Fire Name	Area (acres)	Daily Growth (acres)	NO_x (tons)	VOCs (tons)	rVOCs (tons)	E (tons)[1]	Distance (km)	Q/d (tons/km)[2]	Fuel Loading
Lions[3]	8,484	346	15.42	563.28	338	353	385.0	0.9	Red fir forest
Ferguson[4]	94,992	1,661	37.44	280.61	168	206	450	0.5	CA live oak-blue oak woodland
Donnell[5]	13,814	2,470	110.09	4021.09	2,413	2,523	485	5.2	Red fir forest
Mendocino Complex[6]	300,086	9,394	192.63	6182.35	3,709	3,902	779.31	10.8	Jeffrey pine; ponderosa pine; Douglas fir; CA black oak forest

Note: Growth for all dates shown was obtained from agency estimates available from InciWeb or satellite estimates of growth.

[1] Sum of NO_x and rVOC emissions.
[2] Aggregate Q/d calculated for all fires shown is **10.9** tons/km.
[3] Source: https://web.archive.org/web/20181105223748/https://inciweb.nwcg.gov/incident/5850/
[4] Source: https://goldrushcam.com/sierrasuntimes/index.php/news/local-news/15130-ferguson-fire-near-yosemite-national-park-in-mariposa-county-wednesday-morning-august-8-2018-update-94-992-acres-with-containment-at-43
[5] Source: https://www.fs.usda.gov/detail/stanislaus/news-events/?cid=FSEPRD591425
[6] Source: https://web.archive.org/web/20180809074721/ https://inciweb.nwcg.gov/incident/news/6073

4.3.2.2 Key Factor #2

Figures 4-3 through 4-8 show that O_3 levels on August 6–7 were above the five-year 95th percentile values at all exceeding sites in HA 212, excluding the O_3 level at Palo Verde on August 7. The O_3 exceedances at Paul Meyer and Walter Johnson on August 6 were above the five-year 99th percentile values, and were ranked the first and second highest values in 2018, respectively (Table 1-1). The Key Factor #2 analysis results thus do not completely meet the criteria to support a demonstration that the O_3 exceedance on August 6–7 was caused by an exceptional event, but are strong evidence of the presence of an extreme event.

4.3.2.3 Evidence of Fire Emissions Transport to Area Monitors

Visible Satellite Imagery

Visible satellite imagery from the MODIS Aqua and Terra satellites shows the dense smoke from the Ferguson Fire, Lions Fire, Carr Fire, Donnell Fire, and Mendocino Complex Fire in California on August 6–7 (Figures 4-15 and 4-16). Continuous smoke from wildfires was transported southward/southeastward and eastward during these days; therefore, wildfire emissions dominated the atmosphere in California and Nevada.

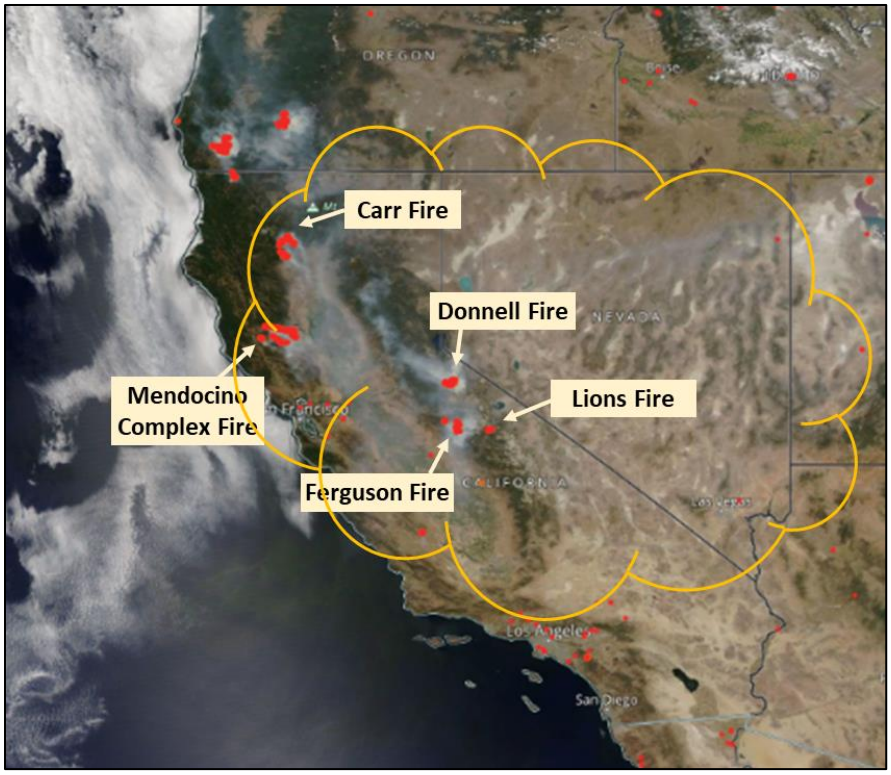

Source: NASA Worldview

Figure 4-15. Visible Satellite Imagery on August 6.

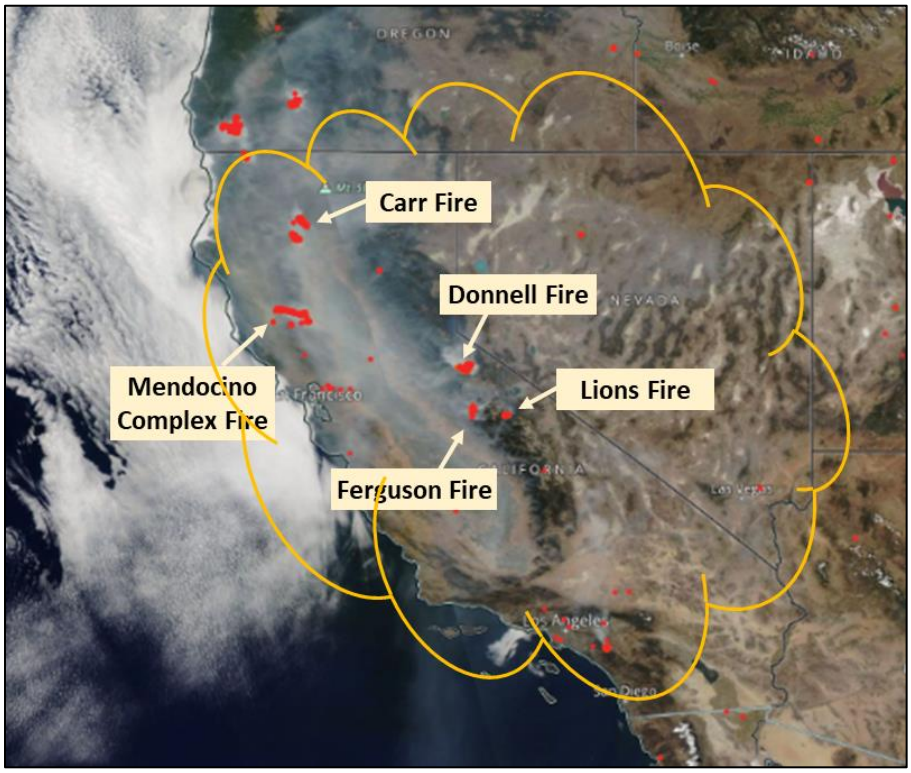

Source: NASA Worldview

Figure 4-16. Visible Satellite Imagery on August 7.

NOAA Daily HMS Smoke Map

The HMS can demonstrate the transport of fire emissions to impacted monitors because HMS smoke plume data is based on measurements from several environmental satellites. The daily HMS smoke maps for August 6–7 in Figures 4-17 and 4-18 show smoke plumes over the western United States, including California and Nevada. They provide evidence of wildfire emissions being transported to monitors in the LVV.

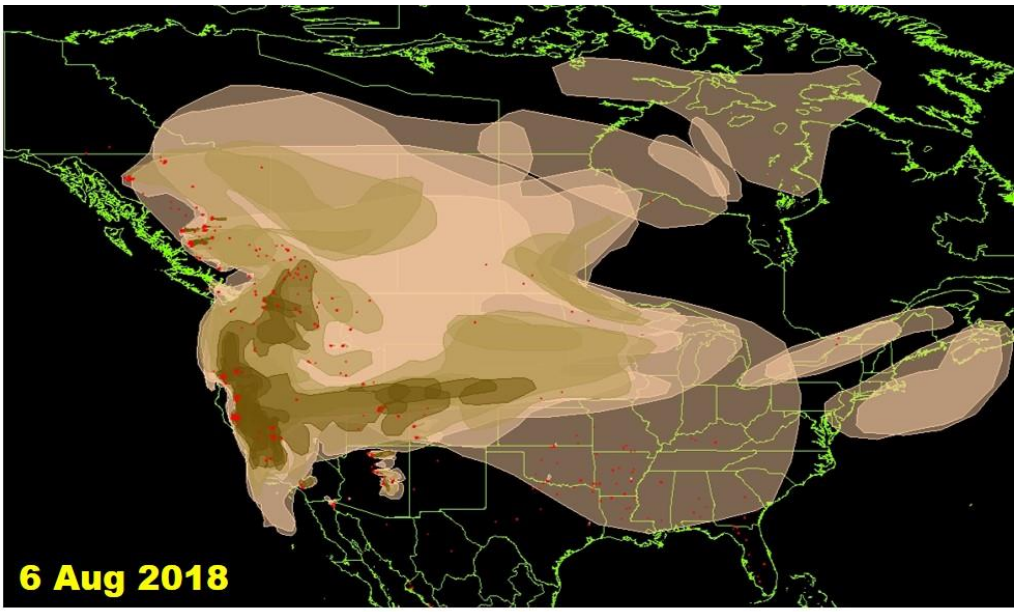

Figure 4-17. NOAA HMS Smoke Analysis, Valid August 6.

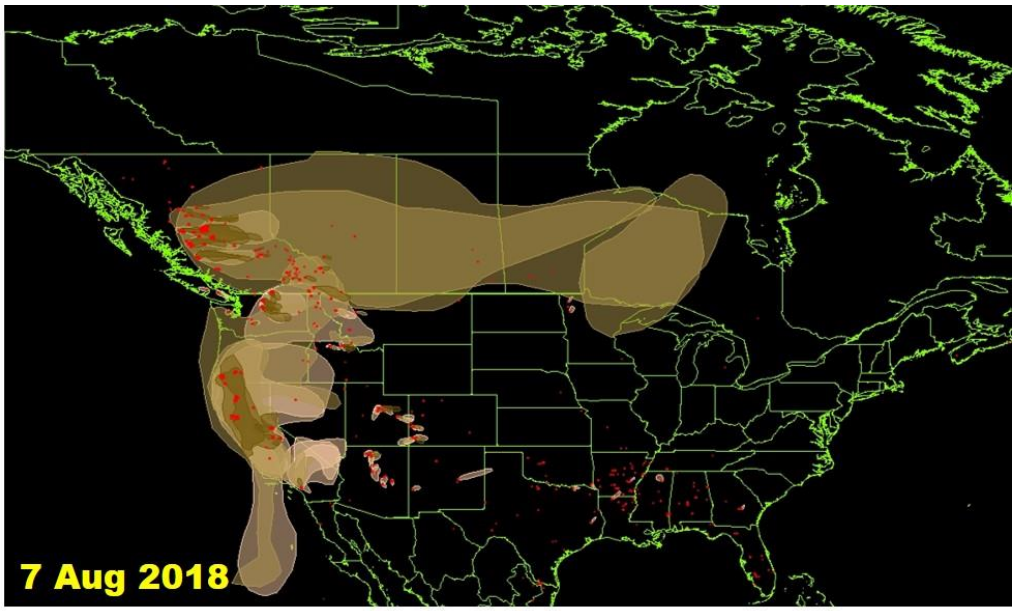

Figure 4-18. NOAA HMS Smoke Analysis, Valid August 7.

Ground Visibility Imagery

Ground images from DES visibility cameras, located on the roof of the M Hotel in Las Vegas, clearly show the smoky conditions that persisted on August 6–7 (Figures 4-17 and 4-18). When compared to images taken on the clear day of May 17, 2018 (Figure 4-19), the August 6–7 images show drastically reduced visibility in the morning and afternoon due to wildfire smoke.

LST = Local Sidereal Time.

Figure 4-19. Visibility Images on a Clear Day (August 6, 2018) at 7 AM (left) and 1 PM (right) LST in Las Vegas.

Figure 4-20. Visibility Images on a Clear Day (August 7, 2018) at 7 AM (left) and 1 PM (right) LST in Las Vegas.

Figure 4-21. Visibility Images on a Clear Day (May 17, 2018) at 7 AM (left) and 1 PM (right) LST in Las Vegas.

Satellite Retrieval—CALIPSO & HYSPLIT Backward Trajectories

We examined the data retrieved from the CALIPSO satellite, launched in June 2006. To make use of this data, we identified the vertical profile of atmospheric aerosols. An examination of CALIPSO's orbital track over the southwest U.S. and the vertical profile of corresponding aerosols (Figures 4-20 and 4-21) suggest the smoke near wildfire sources could rise above 3,000 m.

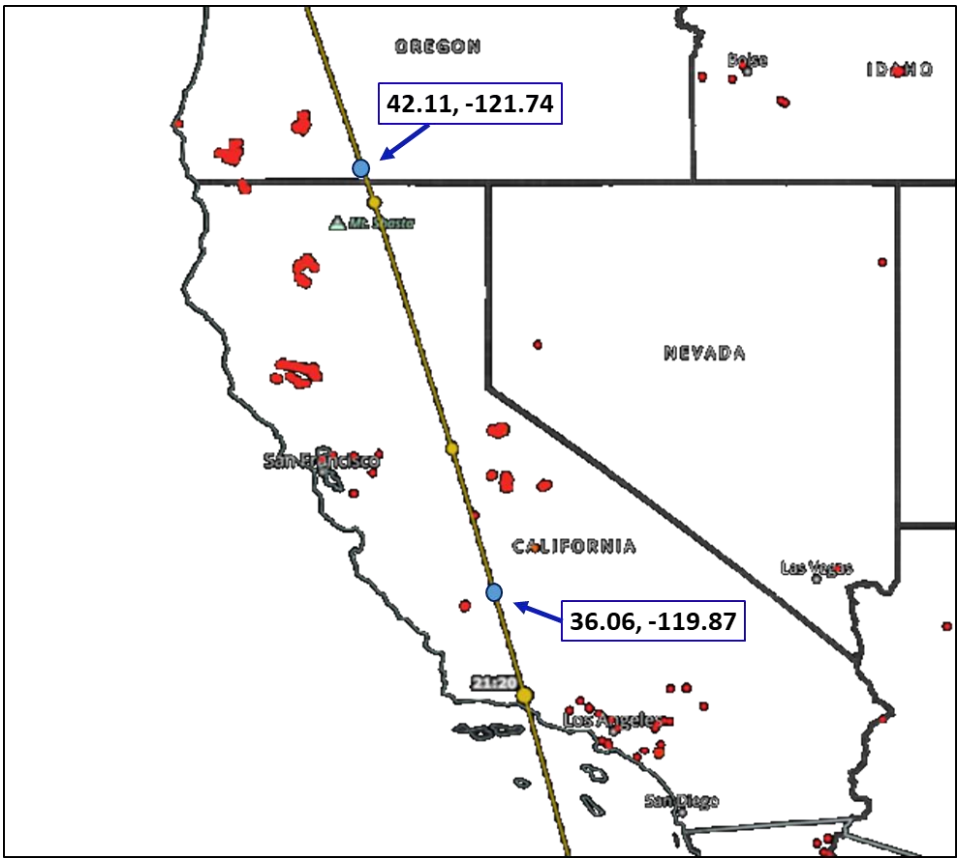

Figure 4-22. CALIPSO Orbital Track over Southwest U.S. on August 6.

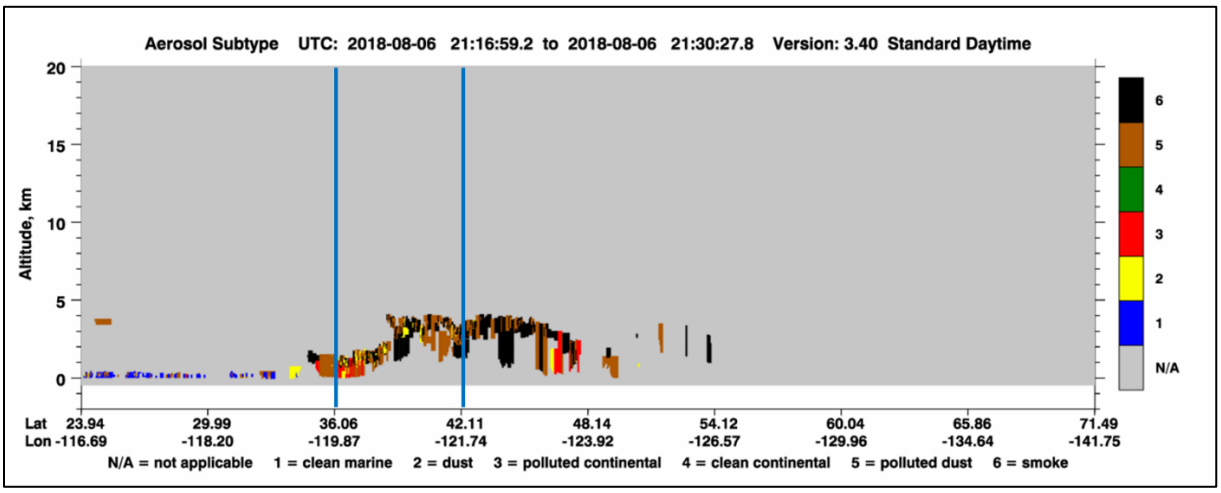

Note: The upper air between two blue lines corresponding to the above blue points on orbital track.

Figure 4-23. CALIPSO Aerosol Type Vertical Profile Collected on August 6.

The NOAA HYSPLIT model was run to produce back trajectories of air parcel movement at 100 m, 1,000 m (Wildfire Guidance recommends within 100~1,500 m), and 3,000 m, according to the plume height in the CALIPSO satellite retrieval data (Figure 4-21), for all six monitors (Green Valley, Jerome Mack, Walter Johnson, Paul Meyer, Palo Verde, and Joe Neal) in HA 212. Figures 4-22 and 4-23 show the 24-hour backward trajectories of airflows arriving at these six monitors on August 6–7 at 1:00 p.m. PST. Figures 4-22 and 4-23 show the air parcel generally traveled from the Mojave Desert to the LVV at a higher level of 1,000 m and 3,000 m and traveled more locally at 100 m, indicating a lack of valley ventilation in the LVV. They show that the air in these areas was affected by, smoke, ozone, and ozone precursor emissions from northern and central California fires (Figures 4-17 and 4-18).

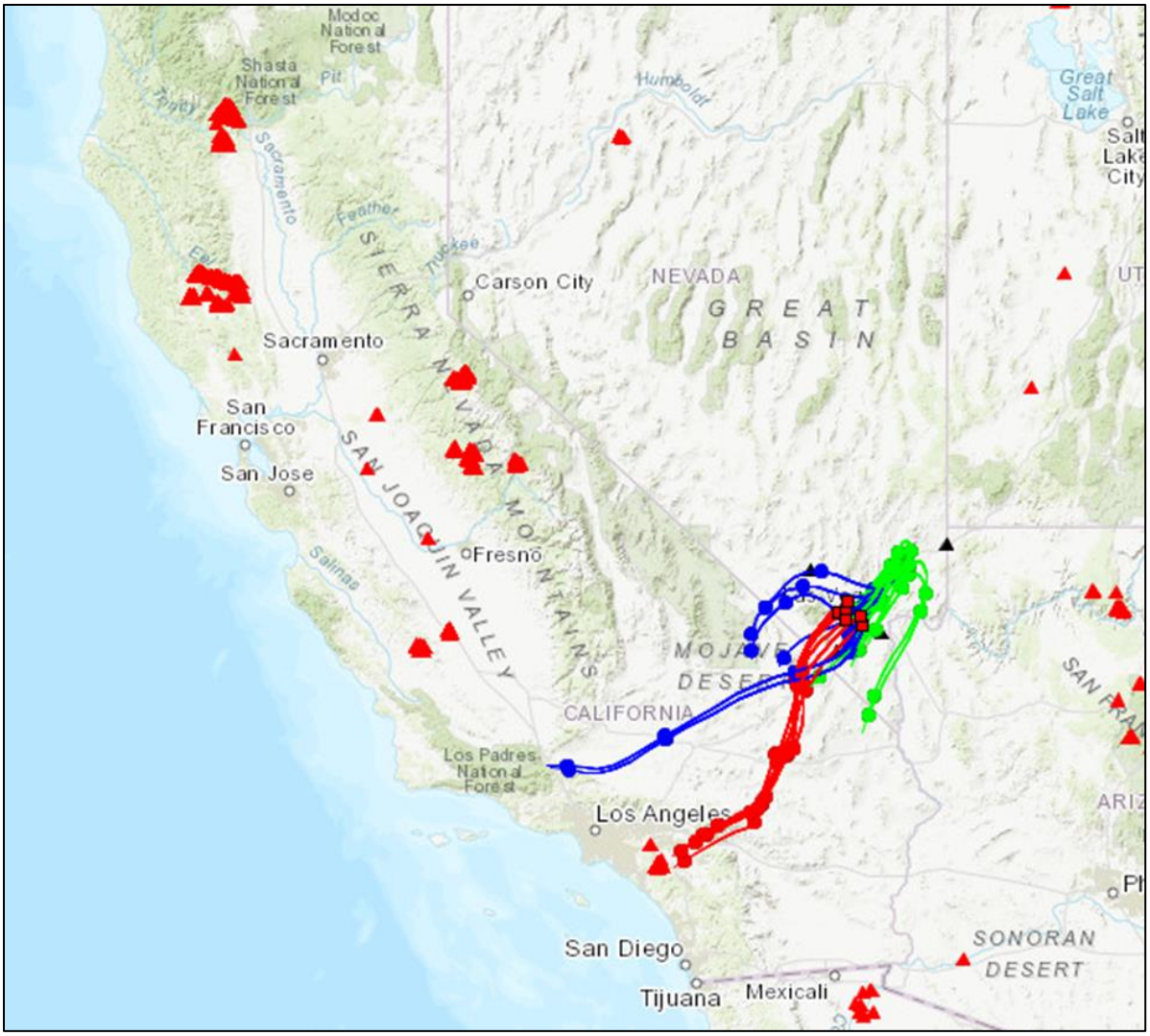

Note: Red = 1000 m, blue = 100 m, green = 10 m.

Figure 4-24. 24-hr Backward Trajectories at Green Valley, Jerome Mack, Walter Johnson, Paul Meyer, Palo Verde, and Joe Neal for August 6.

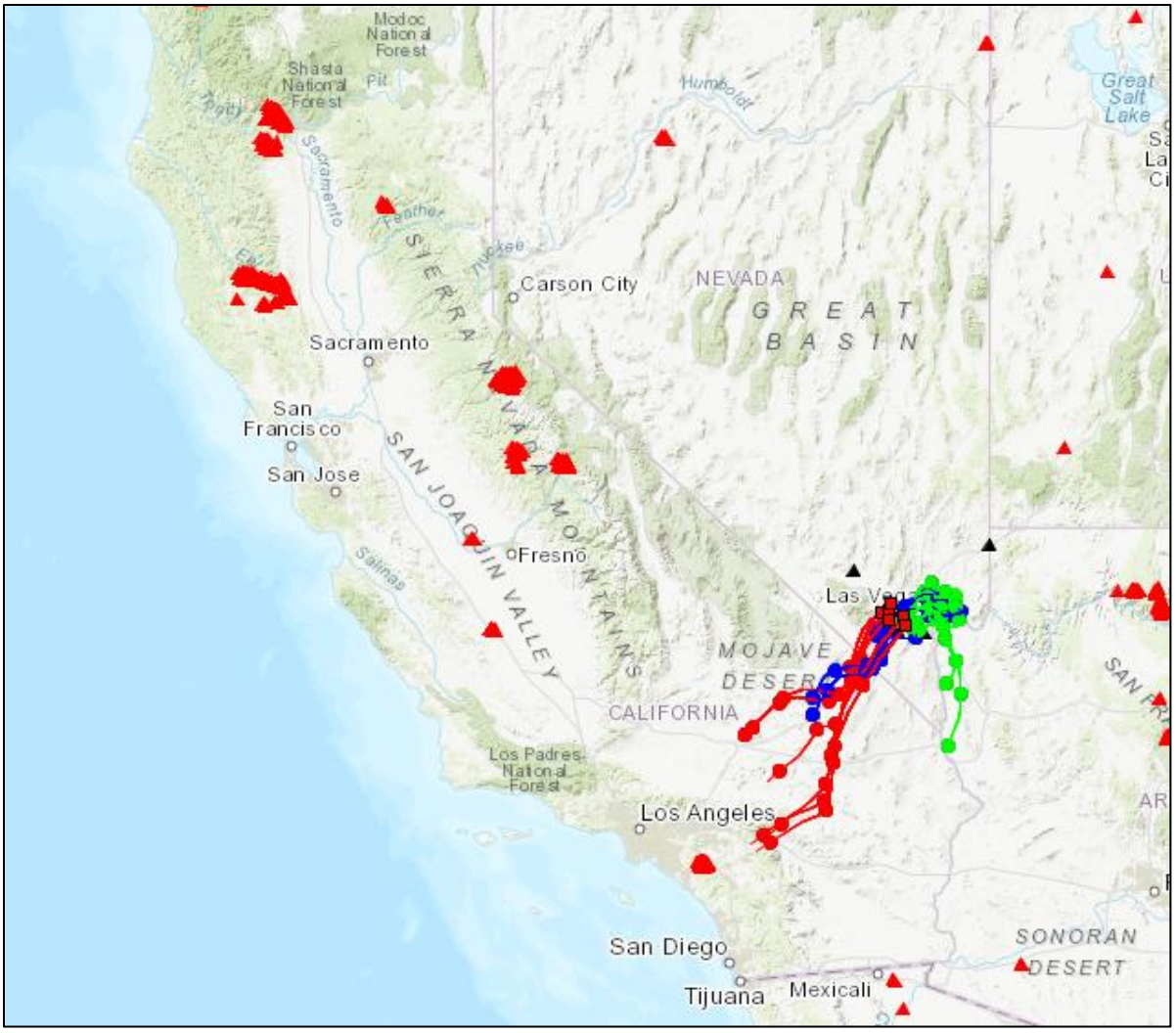

Note: Red = 1000 m, blue = 100 m, green = 10 m.

Figure 4-25. 24-hr Backward Trajectories at Green Valley, Jerome Mack, Walter Johnson, Paul Meyer, Palo Verde, and Joe Neal for August 7.

4.3.2.4 Evidence that Fire Emissions Affected Area Monitors

Concurrent Rise in Ozone Concentrations

We examined MDA8 O_3 at monitors inside (Figure 2-2) and outside (Figure 4-24) the LVV on August 4–8, 2018 (Figures 4-25 and 4-26). Visible satellite imagery, HMS smoke maps, backward trajectories, and the meteorological conditions detailed in Section 3.3 depict the transport of smoke, ozone, and ozone precursor emissions from wildfires in central and northern California to the LVV. The intermittent and widespread smoke appears to have had a significant influence on ozone concentrations, with MDA8 O_3 near/above the 95th percentile value at surrounding sites and sites within the LVV on most days from August 4–8 (Figures 4-25 and 4-26). Under

the stagnant conditions described in the conceptual model (Figure 3-9), the combination of wildfire emissions, ozone precursors, and local emissions elevated ozone concentrations at sites in the LVV above the 2015 ozone NAAQS on August 6–7.

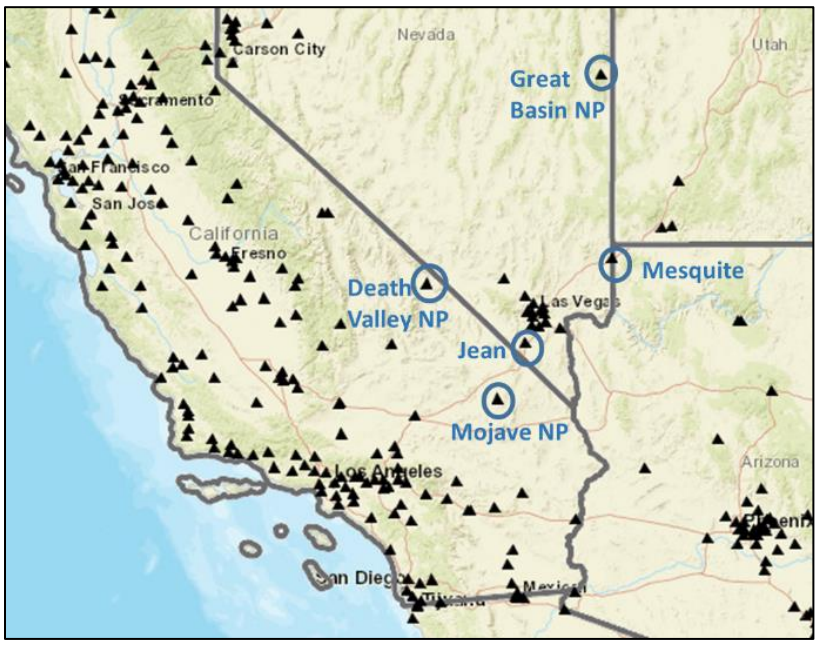

Figure 4-26. Monitors Outside the LVV.

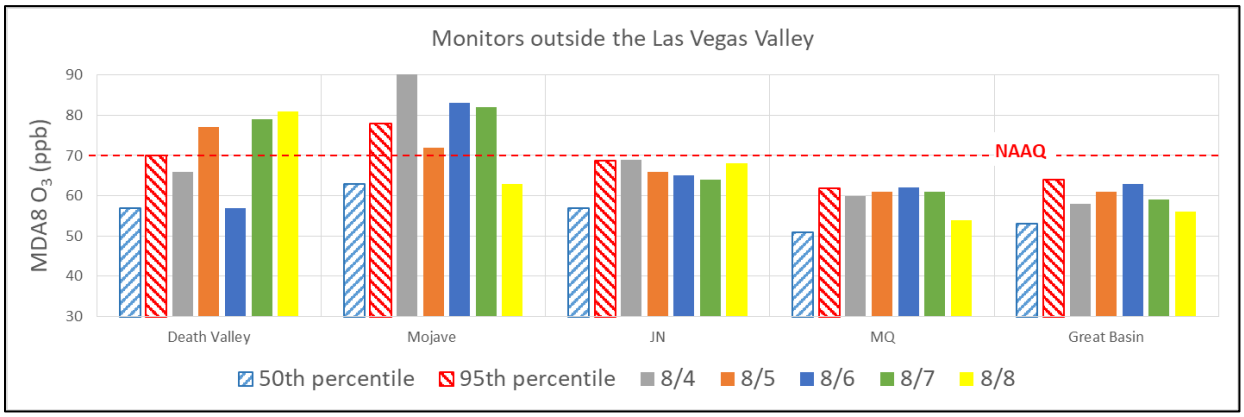

Figure 4-27. MDA8 O_3 at Monitors Outside the LVV, August 4–8.

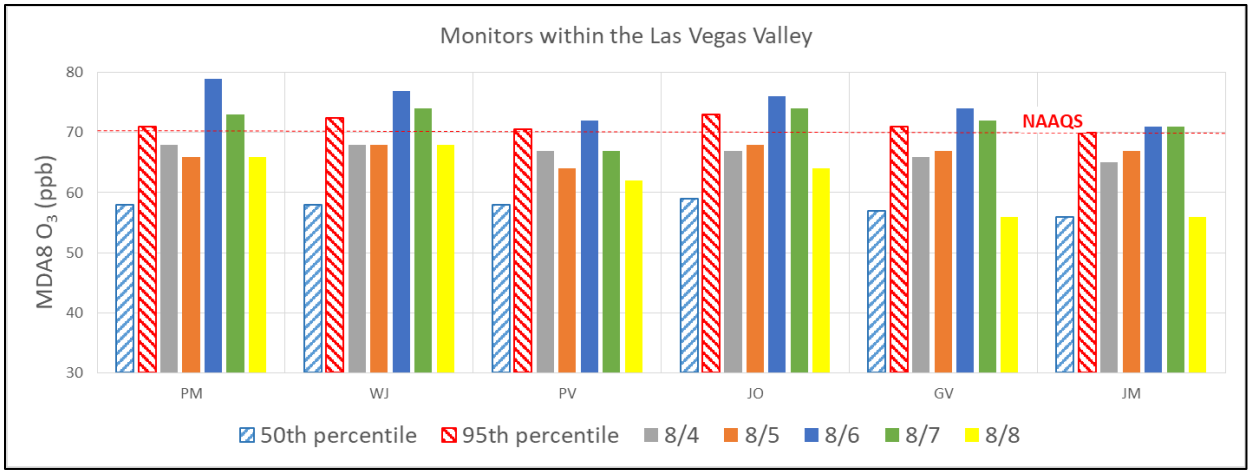

Figure 4-28. MDA8 O_3 at Monitors Inside the LVV, August 4–8.

Analysis of $PM_{2.5}$ Speciation Data

Section 4.2 describes how the ratio of OC to EC can be used to differentiate combustion sources of biomass burning from mobile sources. Figure 4-27 shows the actual and mean OC/EC ratio at Jerome Mack and Rubidoux, CA. It clearly shows that the OC/EC ratio for both sites on August 6 was above their normal summer OC/EC ratio. The results provide evidence the presence of wildfire smoke did influence the levels of ozone in upwind areas and the LVV.

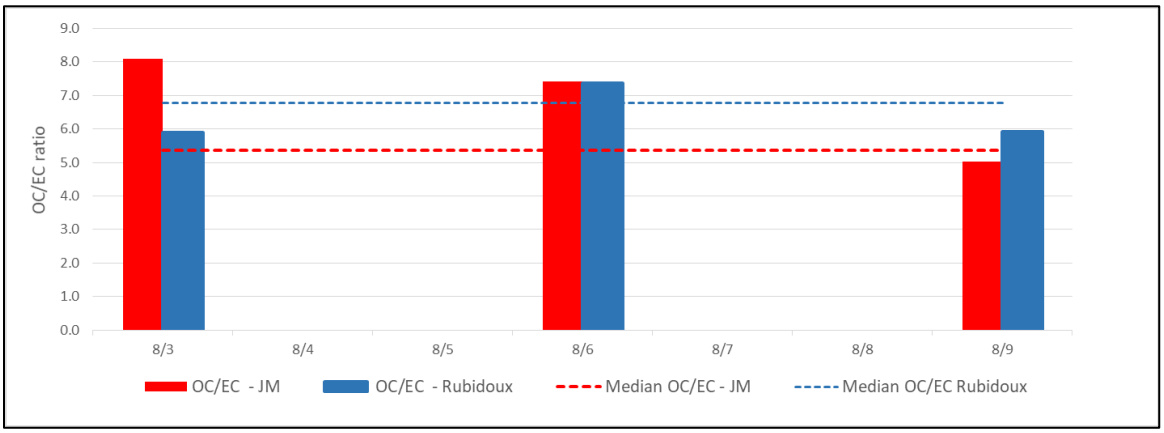

Figure 4-29. Actual and Mean OC/EC ratio at Jerome Mack and Rubidoux, CA, and Daily 24-hour $PM_{2.5}$ at Jerome Mack, August 3-9, 2018.

Analysis of Levoglucosan

The best available $PM_{2.5}$ sample for levoglucosan analysis was collected on August 6. Analysis results were 0.05392 and 0.040875 µg/m^3 for Sunrise Acres and Jerome Mack, respectively, indicating that smoke very likely was present in the LVV on the event day.

Supporting Ground Measurements

Ground measurements of wildfire plume components ($PM_{2.5}$, NO_2, CO) can be used to demonstrate that smoke impacted ground-level air quality if elevated concentrations or unusual diurnal patterns are observed. Jerome Mack is the only monitor that records all four pollutants, and its MDA8 O_3 on August 6–7, 2018, was 71 ppb. Figures 4-28 to 4-31 show hourly levels of O_3, NO_2, $PM_{2.5}$ and CO on August 4–8. These figures clearly show the impact of wildfire smoke on O_3, NO_2, $PM_{2.5}$ and CO concentrations throughout this period, as wildfire smoke was transported intermittently to the LVV. A large increase in O_3 and $PM_{2.5}$ concentrations was seen as early as August 4; however, it was not until August 6 that significant increases in NO_2 and CO concentrations were seen.

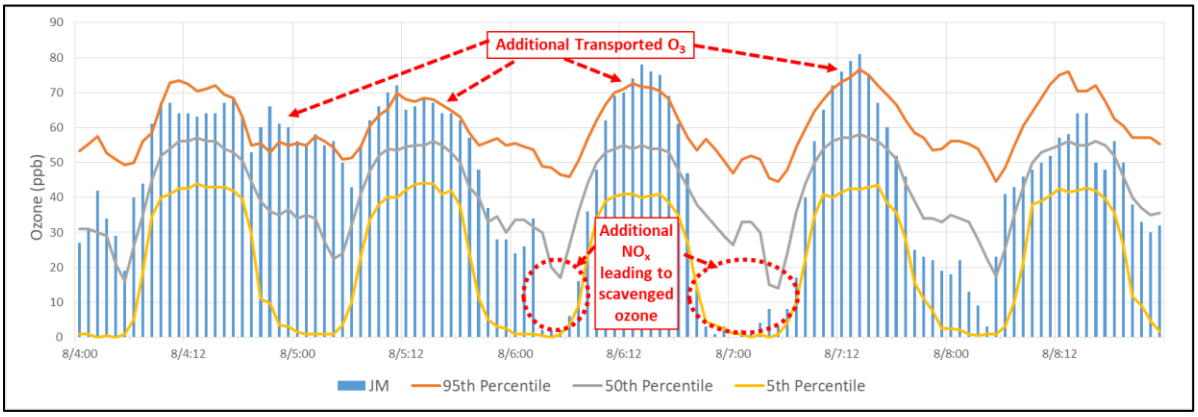

Figure 4-30. Hourly O_3 Concentrations at JM, August 4-8.

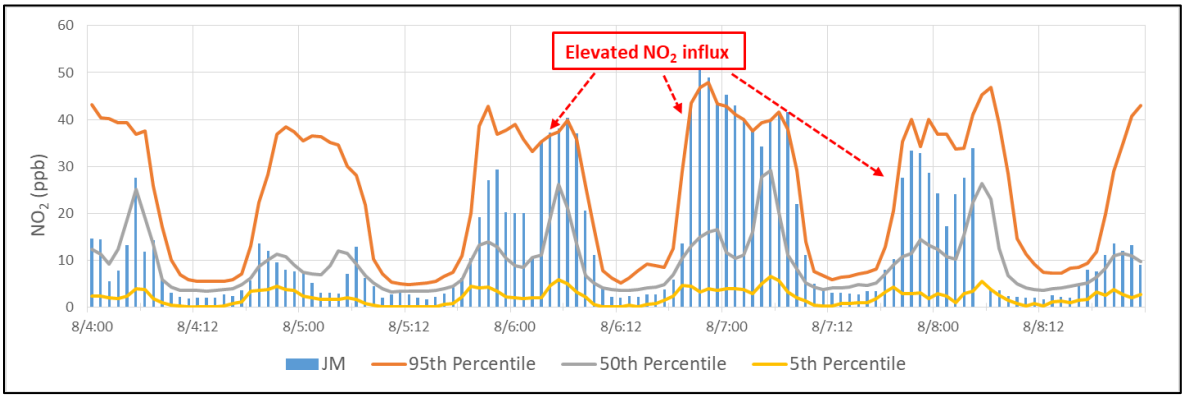

Figure 4-31. Hourly NO_2 Concentrations at JM, August 4-8.

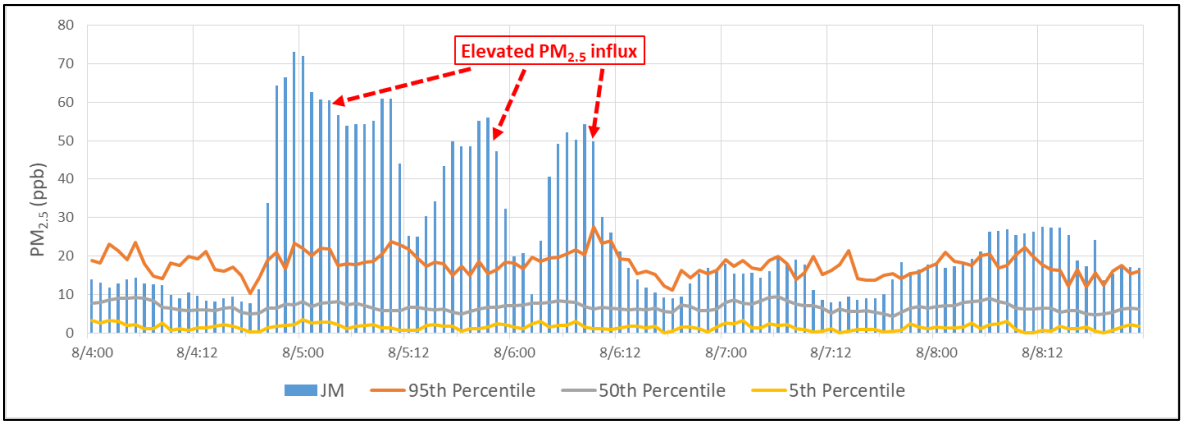

Figure 4-32. Hourly $PM_{2.5}$ Concentrations at JM, August 4-8.

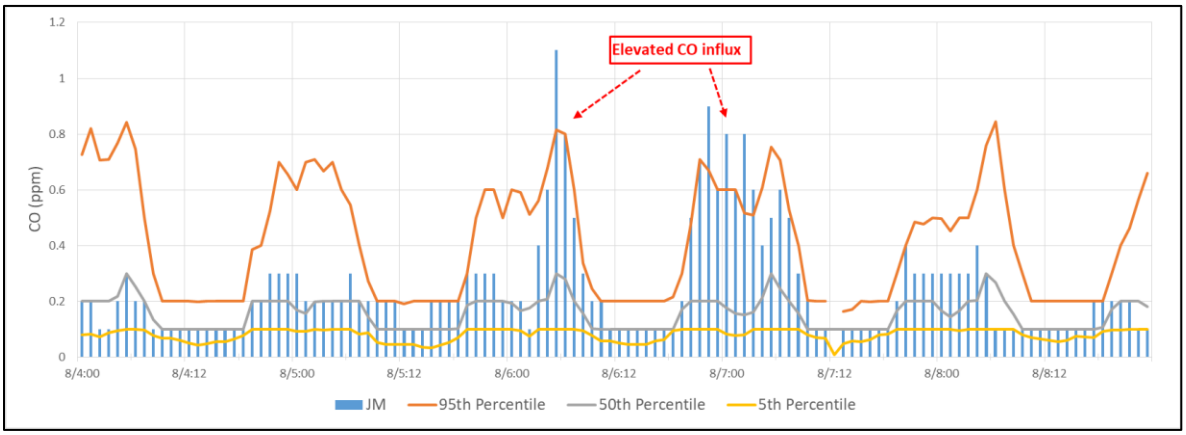

Figure 4-33. Hourly CO Concentrations at JM, August 4-8.

4.3.3 Tier 3 Analysis: Additional Weight of Evidence to Support Clear Causal Relationship

4.3.3.1 GAM Statistical Modeling

Figure 4-32 shows a time series of predicted and observed MDA8 O_3 for August 4–8, 2018. The results indicate the monitors would normally not have exceeded the 2015 NAAQS under the meteorological conditions on August 6–7, suggesting that a variable outside the norm (e.g., increased wildfire emissions) influenced ozone concentrations. Table 4-1 lists GAM results for August 6–7, 2018, at the exceeding monitors petitioned for data exclusion from normal planning and regulatory requirements. GAM residuals show a modeled wildfire impact of between 4.7 and 10.6 ppb for exceeding monitors, with GAM MDA8 O_3 prediction values all below the 70 ppb standard.

EPA guidance recommends using an additional step to estimate the ozone contribution from a wildfire: the difference between the observed ozone and the sum of predicted ozone and the positive 95th percentile value. Simply speaking, the residuals on the wildfire event day would have to

be greater than the positive 95th percentile value to see any wildfire contributions to ozone concentrations. Table 4-1 shows that only the residual for Paul Meyer exceeded the 95th percentile value for August 6. However, two issues with this methodology must be considered.

First, a large number of wildfires affecting Clark County from 2014–2020 (especially in 2018 and 2020) included in GAM modeling cause a very conservative 95th percentile value (positive). Second, given the limitations of regression analysis for ozone production—which involves complex physical and chemical processes regarding emissions and meteorological conditions—models are able to explain about 50% of the correlation between predicted and observed concentrations (see Table 3-16 in *Exceptional Event Demonstration for Ozone Exceedances in Clark County, Nevada—June 22, 2020*), which is typical of the results seen in other regression analysis studies.

The percentile ranks of positive residuals for August 6–7 for the exceeding monitors range from the 65th to 95th and the 64th to 82nd (Table 4-1). The model indicates a 5% ~ 35% and 18% ~ 36% chance that the residuals at exceeding monitors would be produced under the meteorological conditions on August 6–7, suggesting likely additional emissions (e.g., wildfires) were not counted. As Section 3.3 describes, weather conditions on August 6–7 were stable and favored ozone formation. Additional wildfire emissions helped to drive already elevated ozone concentrations to exceed the 2015 NAAQS on August 6-7.

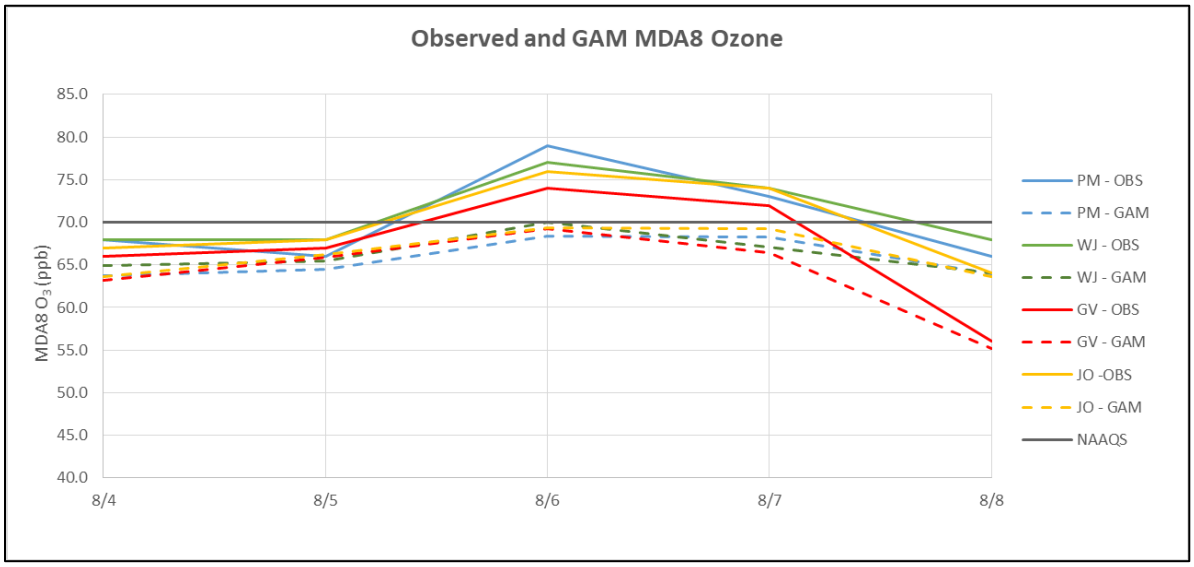

Figure 4-34. Observed and Predicted MDA8 O_3 at Exceeding Monitors, August 4–8.

Table 4-1. August 6-7 GAM Results for Exceeding Sites

Date	Site	MDA8 O_3 (ppb)	MDA8 GAM Prediction (ppb)	GAM Residual (ppb)	Positive 95th Quantile (ppb)	Predicted Fire Influence	Percentile Rank of Positive Residual
8/6/2018	Paul Meyer	79	68.4	10.6	10.5	0.1	95th
	Walter Johnson	77	70.0	7.0	10.8	-3.8	83rd
	Joe Neal	76	69.4	6.6	10.6	-4.0	77th
	Green Valley	74	69.3	4.7	10.1	-5.4	65th
8/7/2018	Paul Meyer	73	68.3	4.7	10.5	-5.8	65th
	Walter Johnson	74	67.1	6.9	10.8	-3.9	82nd
	Joe Neal	74	69.3	4.7	10.6	-5.9	64th
	Green Valley	72	66.5	5.5	10.1	-4.6	73rd

5.0 NATURAL EVENT

40 CFR 50.14(c)(3)(iv)(E) requires that agencies demonstrate an "event was a human activity that is unlikely to recur at a particular location or was a natural event." 40 CFR 50.1(k) defines a natural event as "an event and its resulting emissions, which may recur at the same location, in which human activity plays little or no direct causal role." 40 CFR 50.1(n) defines a wildfire as "any fire started by an unplanned ignition caused by lightning; volcanoes; other acts of nature; unauthorized activity; or accidental, human-caused actions, or a prescribed fire that has developed into a wildfire. A wildfire that predominantly occurs on wildland is a natural event." And lastly, 40 CFR 50.1(o) defines wildland as an "area in which human activity and development are essentially non-existent, except for roads, railroads, power lines, and similar transportation facilities. Structures, if any, are widely scattered."

Based on the documentation provided in Section 3, the event that occurred on August 6-7 falls within the definition of a natural event (40 CFR 50.1(k)). As demonstrated, these wildfires were caused by lighting or human activity and occurred predominantly on wildland, as detailed in Table 5-1, meeting the regulatory definitions outlined in 40 CFR 50.1(n) and (o). DES therefore concludes that these wildfire events can be treated as natural events under the EER.

Table 5-1. Basic Information for Wildfire Event on August 6-7, 2018

Event Date(s)	Fire	Cause	Location–County (State)
August 6-7	Lions Fire	Lightning	Madera (CA)
	Ferguson Fire	Unknown	Mariposa (CA)
	Carr Fire	Human Activity	Shasta/Trinity (CA)
	Mendocino Complex Fire	Human Activity	Colusa, Glenn, Lake, Mendocino (CA)
	Donnell Fire	Unknown	Tuolumne (CA)

6.0 NOT REASONABLY CONTROLLABLE OR PREVENTABLE

Based on the documentation provided in Section 3, lightning and human activity (as defined in 40 CFR 50.1(n)) caused the wildfires on wildland (Table 5-1) that influenced ozone concentrations in the LVV on August 6-7, 2018. DES is not aware of any evidence clearly demonstrating that prevention and control efforts beyond those actually made would have been reasonable; therefore, emissions from these wildfires were not reasonably controllable or preventable.

7.0 CONCLUSIONS

The analyses reported in this document support the conclusion that smoke from wildfires impacted ozone concentrations in Clark County, Nevada, on the event day of August 6-7, 2018. Specifically, this document has used the following evidence to demonstrate the exceptional event:

- Statistical analyses of the monitoring data compared to historical concentrations support the conclusion of unusual and above-normal historical concentrations at monitoring sites.
- Visible satellite imagery, ground visibility imagery, and HMS smoke maps support the conclusion that smoke was transported to LVV monitoring sites.
- Backward trajectories support the conclusion of transport of smoke from wildfires to LVV monitoring sites.
- Enhanced ground measurements of wildfire plume components ($PM_{2.5}$, NO_2, and CO) and OC/EC ratios support the conclusion that ozone concentrations at LVV monitoring sites were impacted by smoke from wildfires.
- Comparisons with non-event concentrations and GAM statistical modeling support the conclusion that the ozone concentrations in Clark County were well above typical summer concentrations.

Based on the evidence presented in this package, the wildfires on August 6–7, 2018, in Clark County were natural events and unlikely to recur. The analyses described satisfy the clear causal relationship criterion for recognition as an exceptional event. Based on this evidence, DES requests that EPA exclude the data recorded at the Green Valley, Joe Neal, Walter Johnson, and Paul Meyer monitors on August 6–7, 2018, from use for regulatory determinations.

8.0 REFERENCES

Bhattarai H., Saikawa E., Wan X., Zhu H., Ram K., Gao S., Kang S., Zhang Q., Zhang Y., Wu G., Wang X., Kawamura K., Fu P., and Cong Z. (2019) Levoglucosan as a tracer of biomass burning: recent progress and perspectives. *Atmospheric Research*, 220, 20-33, doi: 10.1016/j.atmosres.2019.01.004. Available at http://www.sciencedirect.com/science/article/pii/S0169809518311098.

Butler, T.J., Vermeylen F.M., Rury M., Likens G.E., Lee B., Bowker G.E., and McCluney L. 2011. "Response of ozone and nitrate to stationary source NOx emission reductions in the eastern USA." *Atmospheric Environment*, *45*(5), 1084-1094, doi:Doi 10.1016/J.Atmosenv.2010.11.040.

DES. 2008. *Southwest Desert/Las Vegas Ozone Transport Study (SLOTS).* Las Vegas, NV: Clark County Department of Environment and Sustainability.

DES. 2013. *Las Vegas Ozone Study (LVOS)*. Las Vegas, NV: Clark County Department of Environment and Sustainability.

DES. 2017. *Fires, Asia, and Stratospheric Transport Las Vegas Ozone Study (FAST-LVOS).* Las Vegas, NV: Clark County Department of Environment and Sustainability.

Draxler R.R. (1991) The accuracy of trajectories during ANATEX calculated using dynamic model analyses versus rawinsonde observations. *Journal of Applied Meteorology*, 30, 1446-1467, doi: 10.1175/1520-0450(1991)030<1446:TAOTDA>2.0.CO;2, February 25. Available at https://journals.ametsoc.org/downloadpdf/journals/apme/30/10/15200450_1991_030_1446_taotda_2_0_co_2.xml

EPA. 2012. "Our Nation's Air: Status and Trends through 2010." U.S. Environmental Protection Agency, EPA-454/R-12-001. Research Triangle Park, NC: Office of Air Quality Planning and Standards.

EPA. 2016. "Guidance on the Preparation of Exceptional Events Demonstrations for Wildfire Events that May Influence Ozone Concentrations." U.S. Environmental Protection Agency memo. Research Triangle Park, North Carolina.

He, H. et al. 2013. "Trends in emissions and concentrations of air pollutants in the lower troposphere in the Baltimore/Washington airshed from 1997 to 2011." *Atmos. Chem. Phys.*, *13*(15), 7859-7874, doi:10.5194/acp-13-7859-2013.

Hennigan C.J., Sullivan A.P., Collett J.L., Jr., and Robinson A.L. (2010) Levoglucosan stability in biomass burning particles exposed to hydroxyl radicals. *Geophysical Research Letters*, 37(L09806), doi: 10.1029/2010GL043088. Available at https://www.firescience.gov/projects/09-1-03-1/project/09-1-03-1_hennigan_etal_grl_2010.pdf.

Hoffmann D., Tilgner A., Iinuma Y., and Herrmann H. (2009) Atmospheric stability of levoglucosan: a detailed laboratory and modeling study. *Environ. Sci. Technol.*, 44, 694–699.

Jaffe, D.A., Bertschi I., Jaegle L., Novelli P., Reid J.S., Tanimoto H., Vingarzan R., and Westphal D.L. 2004. "Long-range transport of Siberian biomass burning emissions and impact on surface ozone in western North America." *Geophys. Res. Let.*, 31(L16106).

Lai C., Liu Y., Ma J., Ma Q., and He H. (2014) Degradation kinetics of levoglucosan initiated by hydroxyl radical under different environmental conditions. *Atmos. Environ.*, 91, 32-39, doi: 10.1016/j.atmosenv.2014.03.054, 2014/07/01/. Available at http://www.sciencedirect.com/science/article/pii/S1352231014002398.

Lee, S., Baumann, K., Schauer, J.J., Sheesley, R.J., Naeher, L.P., Meinardi, S., Blake, D.R., Edgerton, E.S., Russell, A.G., Clements, M., 2005. "Gaseous and particulate emissions from prescribed burning in Georgia." *Environmental Science and Technology* 39, 9049-9056.

Lee., S., Russell, A.G., 2007. "Estimating uncertainties and uncertainty contributors of CMB PM2.5 source apportionment results." *Atmospheric Environment* 41, 9616-9624.

Lefohn, A., Shadwick D., and Oltmans S. 2010. "Characterizing changes in surface ozone levels in metropolitan and rural areas in the United States for 1980-2008 and 1994-2008." *Atmos. Environ.*, 44, 5199-5210

Nikolov, N. 2008. "Impact of Wildland Fires and Prescribed Burns on Ground Level Ozone Concentration." Paper presented at the Western Regional Air Partnership Workshop on Regional Emissions & Air Quality Modeling Studies, July 30, 2008, Denver, CO.

Pace, T.G., and Pouliot, G. 2007. "EPA's Perspective on Fire Emission Inventories—Past, Present, and Future." Paper presented at the 16th Annual International Emission Inventory Conference (*Emission Inventories: Integration, Analysis, and Communications),* May 14-17, 2007, Raleigh, NC.

Pfister, G.G., Wiedinmyer C., and Emmons L.K. 2008. "Impact of the 2007 California wildfires on surface ozone: integrating local observations with global model simulations." *Geophysical Research Letters*, 35, L19814. doi:10.1029/2008GL034747.

Pio, C.A., Legrand, M., Alves, C.A., Oliveira, T., Afonso, J., Caseiro, A., Puxbaum, H., Sanchez-Ochoa, A., Gelensser, A., 2008. "Chemical composition of atmospheric aerosols during the 2003 summer intense forest fire period." *Atmospheric Environment* 42, 7530-7543.

Rowson, D. and Colucci S. 1992. "Synoptic Climatology of Thermal Low-Pressure Systems over South-Western North America." *International Journal of Climatology*, vol. 12: 529-545.

Sonoma Technology. 2020. "Exceptional Event Demonstration for Ozone Exceedances in Clark County, Nevada—August 18-21, 2020." Section 3.3.2. Petaluma, CA: Sonoma Technology.

Stewart, J., Whiteman C., Steenburgh W., and Bian X. 2002. "A climatological study of thermally driven wind systems of the U.S. intermountain west." *Bulletin of the American Meteorological Society* 83, 699-708

Wood, S.N. 2017. *Generalized Additive Models: An Introduction with R.* 2nd edition. Boca Raton, FL: CRC Press.

Zheng, M., Cass, G.R., Ke, L., Wang, F., Schauer, J.J., Edgerton, E.S., Russell, A.G., 2007. "Source apportionment of daily fine particulate matter at Jefferson street, Atlanta, GA, during summer and winter." *Journal of the Air and Waste Management Association* 57, 228-242.